# 15. SITE 1021[1]

Shipboard Scientific Party[2]

## HOLE 1021A

**Date occupied:** 6 June 1996

**Date departed:** 6 June 1996

**Time on hole:** 07 hr, 45 min

**Position:** 39°5.250′N, 127°46.993′W

**Drill pipe measurement from rig floor to seafloor (m):** 4226.0

**Distance between rig floor and sea level (m):** 11.4

**Water depth (drill pipe measurement from sea level, m):** 4214.6

**Total depth (from rig floor, m):** 4235.5

**Penetration (m):** 9.5

**Number of cores (including cores having no recovery):** 1

**Total length of cored section (m):** 9.5

**Total core recovered (m):** 9.9

**Core recovery (%):** 104.0

**Oldest sediment cored:**
Depth (mbsf): 9.5
Nature: Clay with nannofossils
Age: Quaternary

**Comments:** Overshot the mudline.

## HOLE 1021B

**Date occupied:** 6 June 1996

**Date departed:** 8 June 1996

**Time on hole:** 1 day, 17 hr, 45 min

**Position:** 39°5.248′N, 127°46.985′W

**Drill pipe measurement from rig floor to seafloor (m):** 4222.9

**Distance between rig floor and sea level (m):** 11.4

**Water depth (drill pipe measurement from sea level, m):** 4211.5

**Total depth (from rig floor, m):** 4533.1

**Penetration (m):** 310.2

**Number of cores (including cores having no recovery):** 313

**Total length of cored section (m):** 310.2

**Total core recovered (m):** 311.6

**Core recovery (%):** 100.0

**Oldest sediment cored:**
Depth (mbsf): 310.2
Nature: Clayey diatomite, diatom nannofossil chalk, diatomite with clay
Age: middle Miocene

**Measured velocity (km/s):** 1.6 at Section 33X-1

## HOLE 1021C

**Date occupied:** 8 June1996

**Date departed:** 9 June 1996

**Time on hole:** 21 hr, 45 min

**Position:** 39°5.246′N, 127°46.982′W

**Drill pipe measurement from rig floor to seafloor (m):** 4224.3

**Distance between rig floor and sea level (m):** 11.4

**Water depth (drill pipe measurement from sea level, m):** 4212.9

**Total depth (from rig floor, m):** 4388.4

**Penetration (m):** 164.1

**Number of cores (including cores having no recovery):** 18

**Total length of cored section (m):** 164.1

**Total core recovered (m):** 170.4

**Core recovery (%):** 103.0

**Oldest sediment cored:**
Depth (mbsf):164.1
Nature: Clay with diatoms, nannofossil ooze with clay
Age: late Miocene

## HOLE 1021D

**Date occupied:** 9 June 1996

**Date departed:** 10 June 1996

**Time on hole:** 1 day, 3 hr

**Position:** 39°5.240′N, 127°46.984′W

**Drill pipe measurement from rig floor to seafloor (m):** 4223.8

**Distance between rig floor and sea level (m):** 11.4

**Water depth (drill pipe measurement from sea level, m):** 4212.4

**Total depth (from rig floor, m):** 4362.3

**Penetration (m):** 138.5

**Number of cores (including cores having no recovery):** 15

**Total length of cored section (m):** 138.4

**Total core recovered (m):** 143.8

**Core recovery (%): 103.0**

**Oldest sediment cored:**
Depth (mbsf): 138.5
Nature: Clay, clay with diatoms
Age: early Pliocene

**Principal results:** Site 1021 is the deep-water drill site of the Gorda Transect. It is located about 100 km south of the Mendocino Fracture Zone on 29.6 Ma crust in 4213-m-deep water. The primary drilling objective was to sample the longer term Neogene sedimentary record and use it to study the evolution of the California Current system. Another goal was to develop a correlation between Neogene biostratigraphic data from the northeastern Pacific and the paleomagnetic chronostratigraphy. Site 1021 will also be

[1]Lyle, M., Koizumi, I., Richter, C., et al., 1997. *Proc. ODP, Init. Repts.*, 167: College Station, TX (Ocean Drilling Program).
[2]Shipboard Scientific Party is given in the list preceding the Table of Contents.

used to study preservation of bulk organic matter and, if reliable paleoproductivity indices can be generated, to relate organic matter preservation to flux in low sedimentation-rate environments.

Four holes were cored with the APC/XCB at Site 1021 (Fig. 1) to a maximum depth of 310.1 mbsf, recovering an apparently continuous interval of uppermost middle Miocene to Quaternary (11.8–0 Ma) sediments. Hole 1021A is a 9.5-m-long failed mudline core. Hole 1021B was cored with the APC to 169.5 mbsf and extended with the XCB to a depth of 310.1 mbsf. Hole 1021C was cored with the APC to 164.1 mbsf. Fifteen cores were taken at Hole 1021D with the APC to 138.5 mbsf. Detailed comparisons between the magnetic susceptibility and the GRAPE density record generated on the MST, and high-resolution color reflectance measured with the Oregon State University system, demonstrated complete recovery of the sedimentary sequence down to 185 mcd.

Sediments are dominated either by homogeneous clay-rich intervals or by submeter-scale alternation of calcareous/biosiliceous and siliciclastic strata. All sediments contain biogenic assemblages, mainly calcareous nannofossils, diatoms, foraminifers, and radiolarians, in general order of decreasing abundance. Dominant lithologies are clay, clay with nannofossils, nannofossil ooze, clayey diatomite, and diatom clay mixed sediment. The upper part of the sequence is characterized by a dominance of clay and calcareous nannofossils, whereas diatoms form the main biogenic component in the lower part. Fine-grained volcanic ash layers, and thin clay-rich laminations interpreted as altered ash, serve as potential marker horizons throughout the sequence. The sedimentation rate for the last 10 m.y. was remarkably constant at ~30 m/m.y., but was lower during the late middle Miocene (10–11.8 Ma).

A well-constrained biostratigraphy and chronology are provided by a combination of calcareous nannofossil, planktonic foraminifer, radiolarian and diatom datums, and paleomagnetic reversals (Fig. 1). Radiolarians indicate that the base of Hole 1021B is 11.8 Ma in age.

The microfossil groups are dominated by cool, high-latitude elements from the latest Miocene through the Quaternary. Planktonic foraminifer assemblages are especially cool during Quaternary glacial episodes and the latest Miocene. Radiolarian assemblages suggest relatively warmer conditions during the middle and early late Miocene. Radiolarian species characteristic of upwelling environments are scarce throughout most of the sequence, suggesting weak and episodic vertical advection of deep waters at this location. However, both radiolarians and diatoms indicate that upwelling was stronger during the middle through late Miocene and especially strong during the latest Miocene. Benthic foraminifers indicate that well-oxygenated bottom waters bathed Site 1021 throughout the entire late Neogene.

A complete magnetostratigraphy was determined at Holes 1021B and 1021C after AF demagnetization at 20 mT (Fig. 1). All chrons from the Brunhes (C1n) to the onset of C3n.4n (Thvera subchron) at 5.23 Ma could be identified in the upper 160 mbsf. This section will serve as a well-dated reference for the calibration of biostratigraphic datums.

The organic carbon content is very low and of predominantly marine origin. Concentrations decrease downhole to values that are typical for pelagic sediments. Calcium carbonate concentrations range between 0 and 60 wt%. Intervals of low $CaCO_3$ content are attributed to the dissolution of carbonates. Chemical gradients in the interstitial waters reflect organic matter diagenesis, the dissolution of biogenic opal, and possibly the diffusive influence of reactions in underlying basalt.

Downhole temperature measurements yield a thermal gradient of 54°C/km. Using an average measured thermal conductivity of 0.849 W/(m·K) provides a heat-flow estimate of 46 mW/m$^2$.

## BACKGROUND AND OBJECTIVES

### General Description

Site 1021 is the deepest drill site on Leg 167 and farthest from shore. It is located about 100 km south of the Mendocino Fracture Zone, more than 360 km from the California Coast (Fig. 2). It is situated on an abyssal hill that trends vaguely northwest at a water depth of 4213 mbsl and was chosen for its distance from Delgada Fan deposits (Rea et al., 1985). The age of the ocean crust based upon magnetic anomalies is 29.6 Ma (Atwater and Severinghaus, 1989). The site was surveyed in detail with the *Maurice Ewing* cruise EW9504 in 1995 (Lyle et al., 1995a, 1995b; Fig. 3). The area surveyed for Site 1021 is characterized by a faintly layered sediment column above a strong basement reflector, which we assume is basalt at a depth of 480 ms TWT, or about 385 mbsf.

### Site Objectives

Site 1021, deep water drill site of the Gorda Transect, recovered an uppermost middle Miocene to Quaternary section. Sedimentation rates were ~30 m/m.y. since 10 Ma, similar to the nearby DSDP Site 33, which averaged about 30 m/m.y. (McManus, Burns, et al., 1970). The site is not suitable for very high-resolution paleoceanographic studies, but it was drilled to study the longer term Neogene record. One goal of drilling was to develop a correlation between Neogene biostratigraphic data from the northeastern Pacific and the paleomagnetic chronostratigraphy. Because subtropic and subarctic flora and fauna mix along the coast of California, the detailed biostratigraphy fits imperfectly with schema developed for either the tropics or the subarctic North Pacific. Another important goal of Site 1021 is to provide chronological control for biostratigraphic events in the California Current region through the middle Miocene.

Site 1021 was also drilled to assess the paleoceanographic conditions within the northern region of the California Current. In the modern oceans, Site 1021 is located along the seaward flank of the California Current and should contain a record transitional between that of the California Current and the subtropical gyre. The record from this drill site, especially when combined with records from Sites 1020, 1016, and 1010, will be used to monitor the long-term evolution of the California Current system. Studies from rotary-cored DSDP drill sites and land sections indicate that significant shifts in the strength, or at least the temperature, of the California Current have occurred in the past (Ingle, 1973). Leg 167 drilling will improve our ability to resolve these events.

Geochemical indices of paleoproductivity and microfossil assemblages obtained from Site 1021 will also provide important data on nutrients carried by the California Current. Organic carbon content is relatively low (typically <0.5 wt%) and apparently of predominantly marine origin. This environment provides one of the end-members needed to study preservation of bulk organic matter and of specific organic molecules. If reliable paleoproductivity indices can be generated, it should also be possible to relate organic matter preservation to water-column flux in low sedimentation rate environments.

## OPERATIONS

### Transit from Site 1020 to Site 1021

The 131.0-nmi transit from Site 1020 to Site 1021 was accomplished in 11.75 hr at an average speed of 10.9 kt. A 3.5-kHz precision depth recorder survey was performed while approaching Site 1021. The *JOIDES Resolution* arrived at Site 1021 at 1315 hr on 6 June.

### Hole 1021A

Hole 1021A was spudded at 2000 hr on 6 June. A full barrel prevented establishing an accurate mudline, and the hole was abandoned.

### Hole 1021B

Hole 1021B was spudded at 2100 hr on 6 June. APC Cores 167-1021B-1H through 18H were taken down to 169.5 mbsf with 104.6% recovery (Table 1; see Table 2 on CD-ROM in the back pocket of this

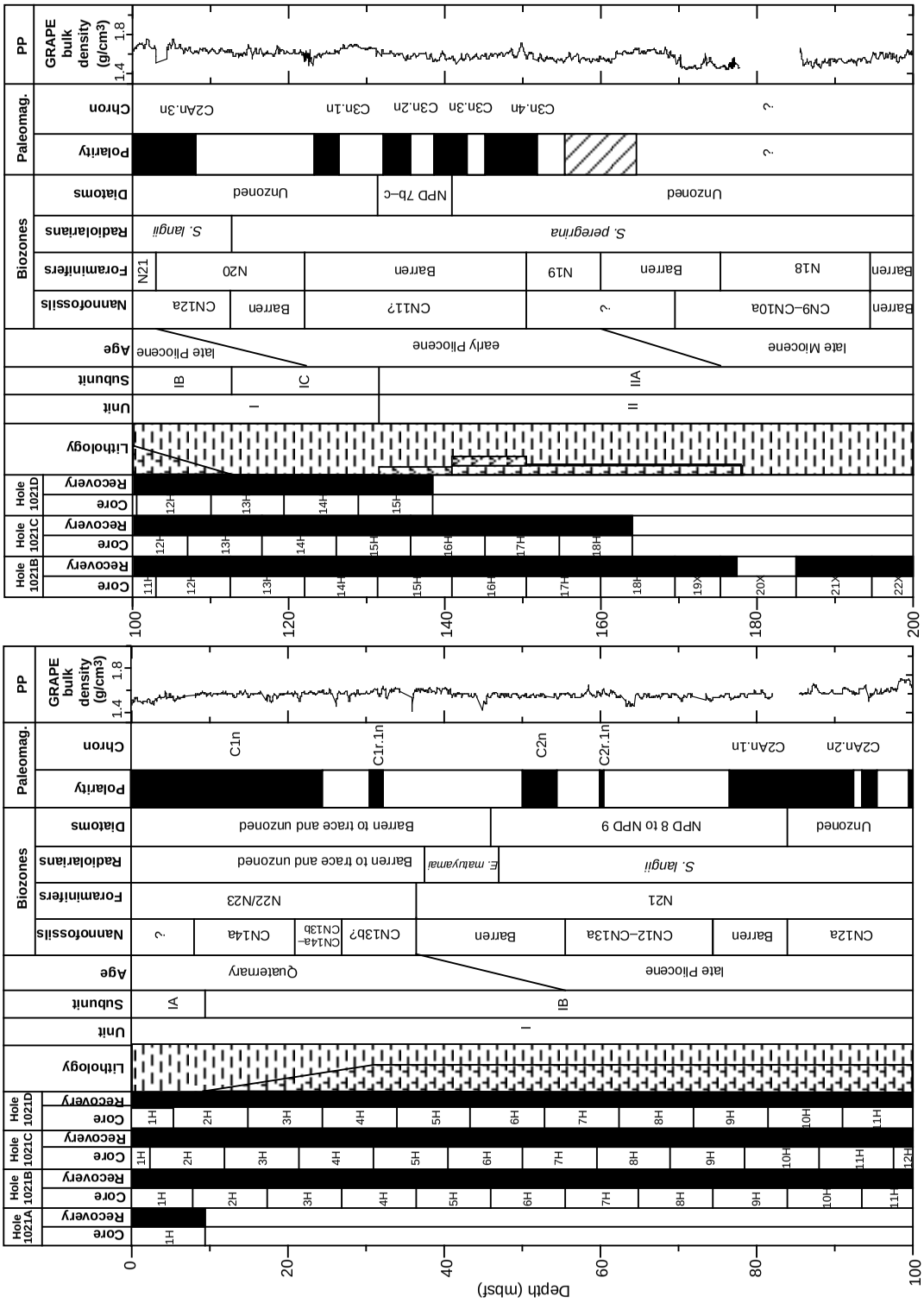


Figure 1. Site 1021 master column.

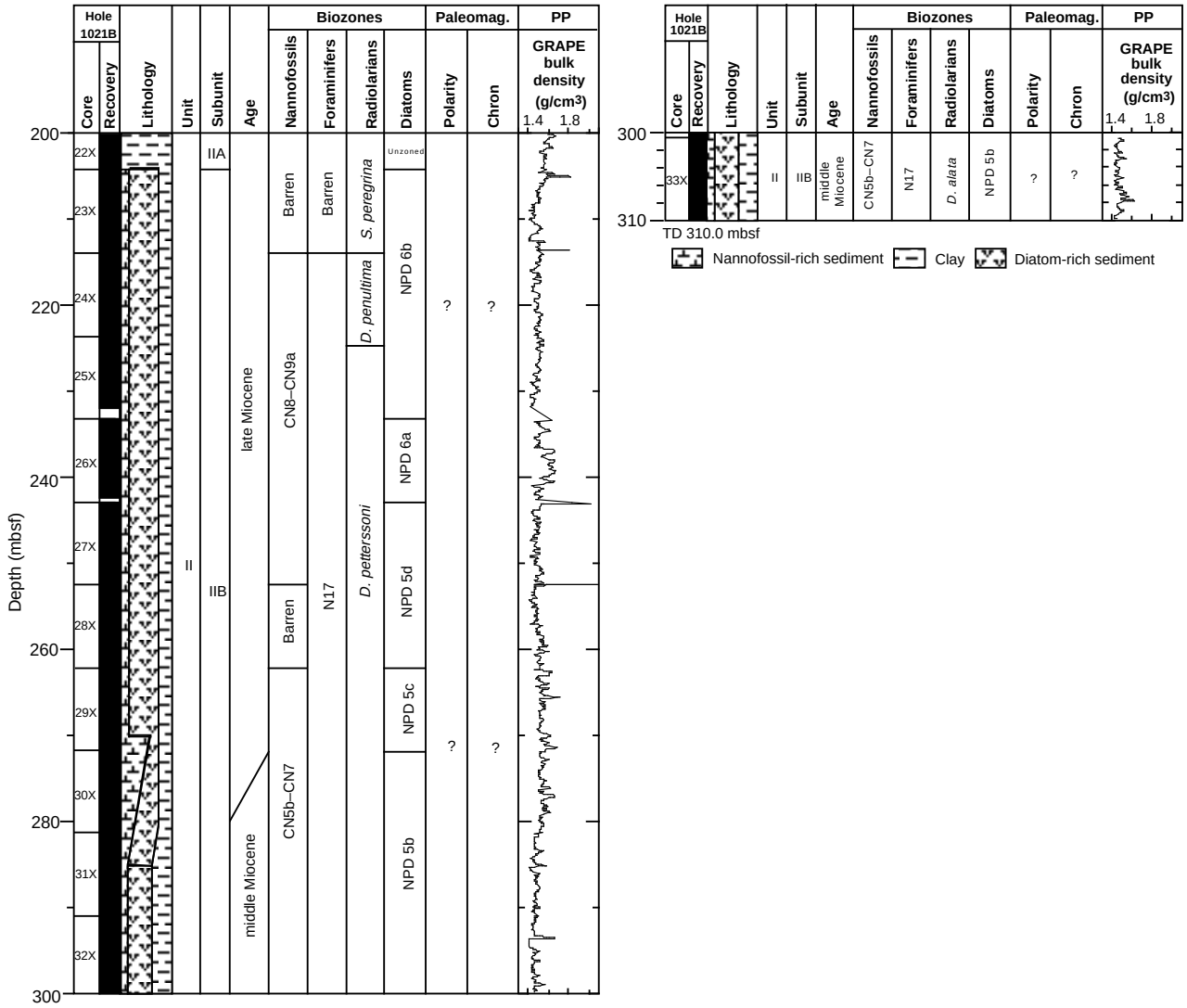


Figure 1 (continued).

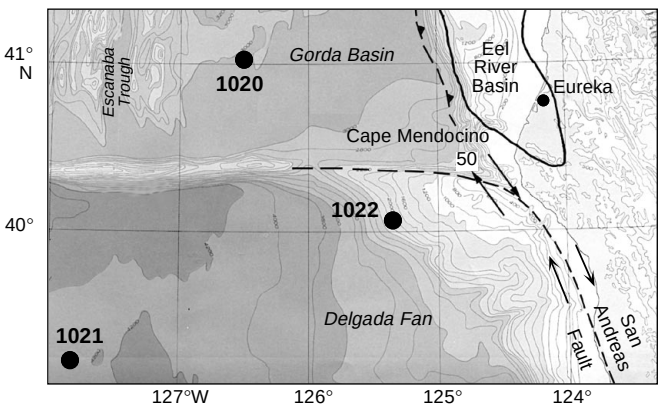


Figure 2. Location map for Site 1021, ~100 km south of the Mendocino Fracture Zone on 29.6 Ma oceanic crust.

volume for a more detailed coring summary). Adara temperature measurements were taken on Cores 167-1021B-4H, 6H, and 9H (see "Physical Properties" section, this chapter). Oriented cores were obtained starting with Core 169-1021B-3H. XCB Cores 167-1021B-19X through 33X were taken down to 310.1 mbsf with 96.1% recovery.

## Hole 1021C

The vessel was offset 10 m to the south and Hole 1021C was spudded at 1545 hr on 8 June. APC Cores 167-1021C-1H through 18H were taken down to 164.1 mbsf with 103.8% recovery (Table 1). Oriented cores were obtained again starting with Core 167-1021C-3H.

## Hole 1021D

The vessel was offset 10 m south and Hole 1021D was spudded at 1330 hr on 9 June. APC Cores 167-1021D-1H through 15H were taken down to 138.5 mbsf with 103.9% recovery (Table 1). The drill string was tripped back to the surface and secured for the 12-hr transit to Site 1022 by 1530 hr on 10 June.

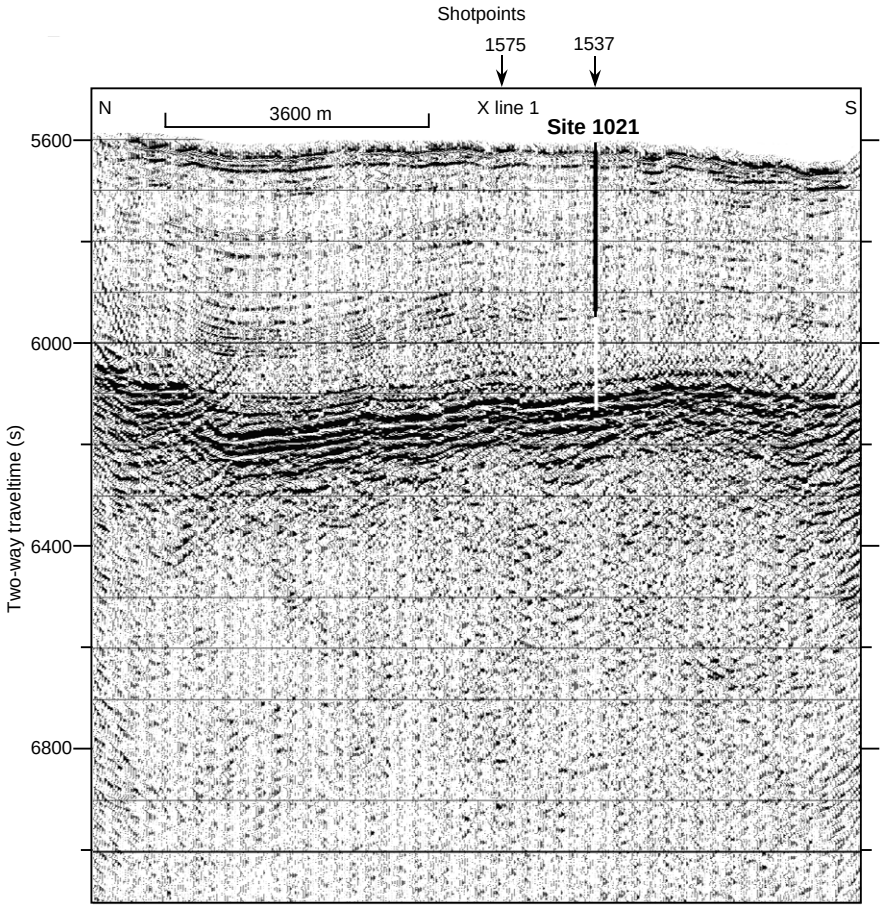


Figure 3. Seismic reflection profile through Site 1021 (Line EW9504 CA5-4; Lyle et al., 1995a, 1995b). The summed 4-channel data were filtered between 30 and 200 Hz, with predictive deconvolution and Stolt F-K migration applied. The profile is roughly along the strike of the abyssal hill on which Site 1021 was drilled. On y-axis, (s) = milliseconds.

## LITHOSTRATIGRAPHY

### Introduction

A nearly continuous, 310.2-m-thick sequence of Miocene to Quaternary (11.8–0 Ma) sediments was recovered at Site 1021. Sediments are dominated either by homogeneous clay-rich intervals or by submeter-scale alternation of carbonate/biosiliceous and siliciclastic strata. All sediments contain biogenic assemblages, mainly calcareous nannofossils, diatoms, foraminifers, and radiolarians, in general order of decreasing abundance. The upper part of the sequence is characterized by a dominance of calcareous nannofossils, whereas diatoms form the main biogenic component in the lower part. Fine-grained volcanic ash layers, and thin clay-rich laminations interpreted as altered ash, serve as potential marker horizons throughout the sequence. The sediments are slightly to moderately bioturbated, with increasing intensity downhole.

The sedimentary succession consists of two distinct Units (I and II) as determined by visual core descriptions and smear-slide estimates. (Fig. 4). Contacts between the two units and five subunits are sharp and based on changes in composition and color. Subunits IA to IC, IIA and IIB are distinguished by different levels of clay, carbonate, and biogenic silica. Increased clay and diatom components contribute to darker colors, whereas light colors are associated with nannofossil oozes.

### Description of Units

#### *Unit I*

Hole 1021A, interval 167-1021A-1H-CC; 0 to 9.5 mbsf (base of hole);
Hole 1021B, interval 167-1021B-1H-1 through 14H-CC; 0 to 131.5 mbsf;
Hole 1021C, interval 167-1021C-1H-1 through 15H-3, 150 cm; 0 to 130.6 mbsf;
Hole 1021D, interval 167-1021D-1H-1 through 15H-4, 60 cm; 0 to 134.1 mbsf.
Age: Quaternary to early Pliocene, 0–4.5 Ma.

Unit I is characterized by an abundance of calcareous nannofossils and clay. Dominant lithologies are clay, clay with nannofossils, nannofossil clay mixed sediment, and nannofossil ooze with clay. Diatoms, foraminifers, and radiolarians are minor components. Colors on freshly cut surfaces vary only moderately from light grayish olive to greenish gray (10Y 5/1 to 10Y 7/1) in the upper part and from light greenish gray to dark greenish gray (5G 6/1 to 5GY 4/1) in the lower part. Color changes are gradual and faintly mottled by bioturbation. Lighter color values correspond to slightly increased nannofossil content, and darker colors correspond to increased clay and/or diatom content. Clay- and silt-sized particles dominate; foraminifers form the rare sand fraction.

The sediment is weakly to locally heavily bioturbated. Reduction halos commonly surround burrows. *Zoophycos* trace fossils are present from 80 mbsf to the base of the unit. Diagenetically modified laminations are rare features at this site (Fig. 5A).

Based on the relative amount of nannofossils vs. clay, Unit I is divided into three subunits.

*Subunit IA*

Hole 1021A, interval 167-1021A-1H-CC; 0 to 9.5 mbsf (base of hole);
Hole 1021B, interval 167-1021B-1H-1 through 1H-CC; 0 to 8.0 mbsf;
Hole 1021C, interval 167-1021C-1H-1 through 2H-3, 150 cm; 0 to 7.1 mbsf;
Hole 1021D, interval 167-1021D-1H-1 through 2H-4, 60 cm; 0 to 10.6 mbsf.
Age: Quaternary, 0–0.35 Ma.

**Table 1. Coring summary for Site 1021.**

| Core | Date (June 1996) | Time | Top (mbsf) | Bottom (mbsf) | Length cored (m) | Length recovered (m) | Recovery |
|---|---|---|---|---|---|---|---|
| 167-1021A- | | | | | | | |
| 1H | 07 | 0320 | 0.0 | 9.5 | 9.5 | 9.86 | 104.0 |
| 167-1021B- | | | | | | | |
| 1H | 07 | 0425 | 0.0 | 8.0 | 8.0 | 7.98 | 99.7 |
| 2H | 07 | 0520 | 8.0 | 17.5 | 9.5 | 9.90 | 104.0 |
| 3H | 07 | 0635 | 17.5 | 27.0 | 9.5 | 9.85 | 103.0 |
| 4H | 07 | 0805 | 27.0 | 36.5 | 9.5 | 9.83 | 103.0 |
| 5H | 07 | 0915 | 36.5 | 46.0 | 9.5 | 9.87 | 104.0 |
| 6H | 07 | 1030 | 46.0 | 55.5 | 9.5 | 9.98 | 105.0 |
| 7H | 07 | 1130 | 55.5 | 65.0 | 9.5 | 10.07 | 106.0 |
| 8H | 07 | 1240 | 65.0 | 74.5 | 9.5 | 10.10 | 106.3 |
| 9H | 07 | 1415 | 74.5 | 84.0 | 9.5 | 10.23 | 107.7 |
| 10H | 07 | 1520 | 84.0 | 93.5 | 9.5 | 10.04 | 105.7 |
| 11H | 07 | 1630 | 93.5 | 103.0 | 9.5 | 9.62 | 101.0 |
| 12H | 07 | 1740 | 103.0 | 112.5 | 9.5 | 10.03 | 105.6 |
| 13H | 07 | 2100 | 112.5 | 122.0 | 9.5 | 9.88 | 104.0 |
| 14H | 07 | 2205 | 122.0 | 131.5 | 9.5 | 9.88 | 104.0 |
| 15H | 07 | 2320 | 131.5 | 141.0 | 9.5 | 10.06 | 105.9 |
| 16H | 08 | 0030 | 141.0 | 150.5 | 9.5 | 10.00 | 105.2 |
| 17H | 08 | 0145 | 150.5 | 160.0 | 9.5 | 10.09 | 106.2 |
| 18H | 08 | 0250 | 160.0 | 169.5 | 9.5 | 9.88 | 104.0 |
| 19X | 08 | 0410 | 169.5 | 175.4 | 5.9 | 7.43 | 126.0 |
| 20X | 08 | 0500 | 175.4 | 185.0 | 9.6 | 2.10 | 21.9 |
| 21X | 08 | 0600 | 185.0 | 194.7 | 9.7 | 9.71 | 100.0 |
| 22X | 08 | 0705 | 194.7 | 204.3 | 9.6 | 9.57 | 99.7 |
| 23X | 08 | 0830 | 204.3 | 214.0 | 9.7 | 9.70 | 100.0 |
| 24X | 08 | 0940 | 214.0 | 223.6 | 9.6 | 9.74 | 101.0 |
| 25X | 08 | 1050 | 223.6 | 233.2 | 9.6 | 8.43 | 87.8 |
| 26X | 08 | 1200 | 233.2 | 242.8 | 9.6 | 9.34 | 97.3 |
| 27X | 08 | 1330 | 242.8 | 252.4 | 9.6 | 9.72 | 101.0 |
| 28X | 08 | 1440 | 252.4 | 262.1 | 9.7 | 9.72 | 100.0 |
| 29X | 08 | 1600 | 262.1 | 271.7 | 9.5 | 9.78 | 102.0 |
| 30X | 08 | 1730 | 271.7 | 281.3 | 9.6 | 9.69 | 101.0 |
| 31X | 08 | 1845 | 281.3 | 290.9 | 9.6 | 9.89 | 103.0 |
| 32X | 08 | 1945 | 290.9 | 300.5 | 9.6 | 9.88 | 103.0 |
| 33X | 08 | 2045 | 300.5 | 310.2 | 9.7 | 9.63 | 99.3 |
| 167-1021C- | | | | | | | |
| 1H | 08 | 2300 | 0.0 | 2.6 | 2.6 | 2.59 | 99.6 |
| 2H | 09 | 0005 | 2.6 | 12.1 | 9.5 | 9.98 | 105.0 |
| 3H | 09 | 0120 | 12.1 | 21.6 | 9.5 | 9.61 | 101.0 |
| 4H | 09 | 0220 | 21.6 | 31.1 | 9.5 | 9.90 | 104.0 |
| 5H | 09 | 0320 | 31.1 | 40.6 | 9.5 | 10.07 | 106.0 |
| 6H | 09 | 0420 | 40.6 | 50.1 | 9.5 | 9.98 | 105.0 |
| 7H | 09 | 0520 | 50.1 | 59.6 | 9.5 | 9.82 | 103.0 |
| 8H | 09 | 0620 | 59.6 | 69.1 | 9.5 | 9.73 | 102.0 |
| 9H | 09 | 0730 | 69.1 | 78.6 | 9.5 | 9.70 | 102.0 |
| 10H | 09 | 0900 | 78.6 | 88.1 | 9.5 | 9.91 | 104.0 |
| 11H | 09 | 1005 | 88.1 | 97.6 | 9.5 | 9.94 | 104.0 |
| 12H | 09 | 1115 | 97.6 | 107.1 | 9.5 | 10.01 | 105.3 |
| 13H | 09 | 1230 | 107.1 | 116.6 | 9.5 | 9.86 | 104.0 |
| 14H | 09 | 1315 | 116.6 | 126.1 | 9.5 | 9.88 | 104.0 |
| 15H | 09 | 1455 | 126.1 | 135.6 | 9.5 | 9.93 | 104.0 |
| 16H | 09 | 1655 | 135.6 | 145.1 | 9.5 | 9.98 | 105.0 |
| 17H | 09 | 1725 | 145.1 | 154.6 | 9.5 | 9.64 | 101.0 |
| 18H | 09 | 1830 | 154.6 | 164.1 | 9.5 | 9.86 | 104.0 |
| 167-1021D- | | | | | | | |
| 1H | 09 | 2050 | 0.0 | 5.5 | 5.5 | 5.45 | 99.1 |
| 2H | 09 | 2140 | 5.5 | 15.0 | 9.5 | 9.80 | 103.0 |
| 3H | 09 | 2235 | 15.0 | 24.5 | 9.5 | 9.85 | 103.0 |
| 4H | 09 | 2330 | 24.5 | 34.0 | 9.5 | 9.84 | 103.0 |
| 5H | 10 | 0025 | 34.0 | 43.5 | 9.5 | 9.81 | 103.0 |
| 6H | 10 | 0110 | 43.5 | 53.0 | 9.5 | 9.97 | 105.0 |
| 7H | 10 | 0200 | 53.0 | 62.5 | 9.5 | 9.87 | 104.0 |
| 8H | 10 | 0325 | 62.5 | 72.0 | 9.5 | 10.05 | 105.8 |
| 9H | 10 | 0425 | 72.0 | 81.5 | 9.5 | 9.95 | 105.0 |
| 10H | 10 | 0515 | 81.5 | 91.0 | 9.5 | 9.95 | 105.0 |
| 11H | 10 | 0630 | 91.0 | 100.5 | 9.5 | 10.06 | 105.9 |
| 12H | 10 | 0730 | 100.5 | 110.0 | 9.5 | 10.04 | 105.7 |
| 13H | 10 | 0835 | 110.0 | 119.5 | 9.5 | 9.89 | 104.0 |
| 14H | 10 | 0940 | 119.5 | 129.0 | 9.5 | 9.52 | 100.0 |
| 15H | 10 | 1100 | 129.0 | 138.5 | 9.5 | 9.79 | 103.0 |

Note: Table 2, on the CD-ROM in the back pocket, this volume, is a more detailed coring summary.

Clay is the dominant lithology of Subunit IA. The color varies between light grayish olive (10Y 5/2) and pale olive (10Y 6/1) with gradational color changes. The sediment is moderately bioturbated and diagenetic halos commonly surround burrows. The upper part of Subunit IA is characterized by abundant organic debris (up to 10%), hence colors vary around reddish brown to dark yellowish brown (5YR 3/4 to 10YR 4/3).

Thin laminae (<1 cm) of dark greenish gray (10Y 4/2) clay with sharp basal contacts are a frequent minor lithology.

*Subunit IB*

Hole 1021B, interval 167-1021B-2H-1 through 13H-2, 100 cm; 8.0 to 115.0 mbsf;

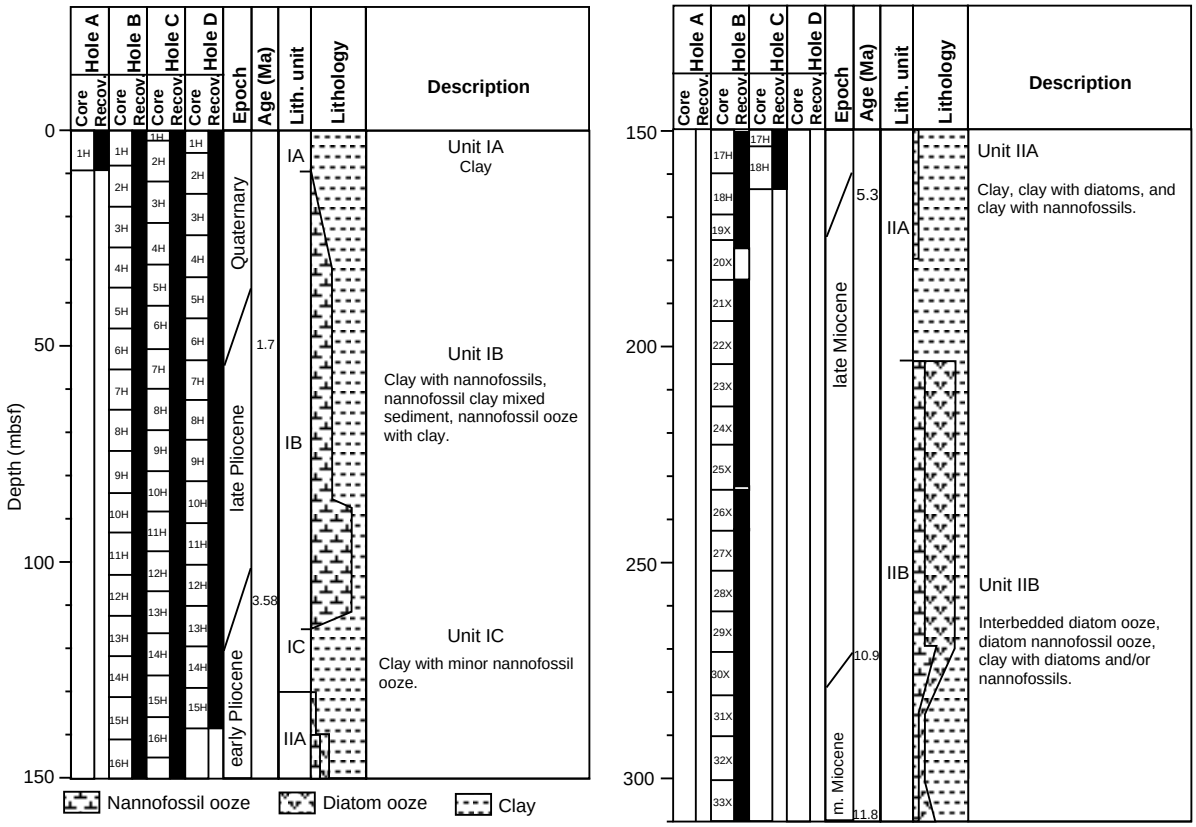


Figure 4. Site 1021 lithostratigraphic summary (0–310.2 mbsf).

Hole 1021C, interval 167-2H-3, 150 cm, through 13H-6, 70 cm; 7.1 to 115.2 mbsf;
Hole 1021D, interval 167-1021D-2H-4, 60 cm, through 13H-4, 75 cm; 10.6 to 115.25 mbsf.
Age: late Pleistocene, 0.35–3.9 Ma.

Subunit IB is characterized by the abundance of calcareous nannofossils (coccoliths dominate strongly over discoasters). Dominant lithologies are clay with nannofossils, nannofossil clay mixed sediment, and nannofossil ooze with clay, all with subtle, gradational contacts. Diatoms, foraminifers, and radiolarians are minor components. The color varies between light grayish olive (10Y 5/1,2) and pale olive (10Y 6/1) with gradational transitions.

The sediment is slightly bioturbated and mottled to heavily bioturbated. Redox patches and haloes around burrows are common, as are *Zoophycos* trace fossils. Burrows are filled with dark gray (N3) soupy mud in the upper part of the interval.

Thin layers (<1 cm) of dark greenish gray (10Y 4/2) clay or dark gray (N 4) color bands are frequently intercalated with the main lithology. Volcanic glass and vitric ash occur occasionally in thin layers. Two small dolomite concretions occur in the lower part of Section 5H-3. Millimeter-scale black laminations are well developed in several places, but appear to be diagenetic features.

*Subunit IC*

Hole 1021B, interval 167-1021B-13H-2, 100 cm, through 14H-CC; 115.0 to 131.5 mbsf;
Hole 1021C, interval 167-1021C-13H-6, 70 cm, through 15H-3, 150 cm; 115.2 to 130.6 mbsf;
Hole 1021D, interval 167-1021D-13H-4, 75 cm, through 15H-4, 60 cm; 115.25 to 134.1 mbsf.
Age: early Pliocene, 3.9–4.5 Ma

As in Subunit IA, Subunit IC is characterized by the dominance of clay with only minor contributions of calcareous nannofossils. Dominant lithologies include dark greenish gray to light greenish gray (5GY 4/1 to 5G 6/1) clay and nannofossil clay. The sediment is generally mottled to slightly bioturbated. Reduction haloes and mottles are common. Pyrite concretions are rare diagenetic features.

***Unit II***

Hole 1021B, interval 167-1021B-15H through 33X-CC (base of hole); 131.5 to 310.2 mbsf;
Hole 1021C, interval 167-1021C-15H-4 through 18H-CC (base of hole); 130.6 to 164.1 mbsf;
Hole 1021D, interval 167-1021D-15H-4, 60 cm, through 15H-CC (base of hole); 134.1 to 138.5 mbsf.
Age: early Pliocene to middle Miocene, 4.5–11.8 Ma.

Unit II is characterized by clay and the increased abundance of diatoms in conjunction with lesser amounts of calcareous nannofossils. The top of Unit II is sharply defined by the appearance of >10% diatoms.

Dominant lithologies are clay with diatoms, diatom clay, diatom ooze, nannofossil ooze, nannofossil clay, clay with diatoms/nannofossils (5GY 5/1 to 10Y 4/2). The sediment is moderately to heavily bioturbated and shows prominent color banding with gradational contacts on a 10-cm to submeter scale. This color banding is particularly well pronounced in the lower part of the unit.

*Subunit IIA*

Hole 1021B, interval 167-1021B-15H through 22X-CC; 131.5 to 204.3 mbsf;
Hole 1021C, interval 167-1021C-15H-4 through 18H-CC (base of hole); 130.6 to 164.1 mbsf;

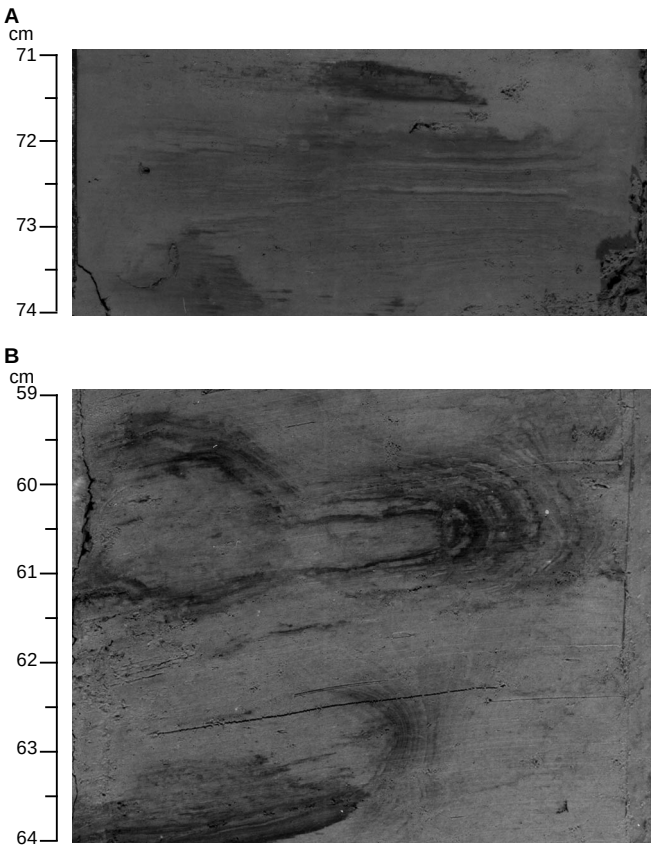


Figure 5. **A.** Millimeter-scale, diagenetically modified laminations at interval 167-1021B-12H-6, 71–74 cm. **B.** Liesegang-type reduction haloes around burrows at interval 167-1021B-18H-3, 59–64 cm.

Hole 1021D, interval 167-1021D-15H-4, 60 cm, through 15H-CC (base of hole); 134.1 to 138.5 mbsf.
Age: early Pliocene to late Miocene, 4.5–7.5 Ma.

Subunit IIA is dominated by clay-rich sediments variously admixed with small amounts (<20% by smear-slide analysis) of diatoms and calcareous nannofossils. Dominant lithologies are clay, clay with diatoms and clay with nannofossils. Colors are dark greenish gray to light greenish gray (5GY 4/1 to 5G 6/1). All contacts are gradational. The general appearance of the sediment is homogeneous to mottled (including reduction mottles) or heavily bioturbated (e.g., *Zoophycos*). Diagenetic color banding is common.

Minor lithologies include thin layers of volcanic glass, dark gray (N4 to N5) vitric ash, and dark green layers of altered volcanic ash.

*Subunit IIB*

Hole 1021B, interval 167-1021B-23X through 33X-CC (base of hole); 204.3 to 310.2 mbsf.
Age: middle Miocene to late Miocene, 7.5–11.8 Ma.

Subunit IIB is characterized by abundant diatom-rich sediments and distinct color banding on a decimeter to meter scale. Color banding is produced by alternation between the dominant lithologies: diatom ooze, diatom nannofossil ooze and clay with diatoms or nannofossils. Colors vary between olive (5Y 5/4) to light olive yellowish gray (10Y 7/1) and greenish gray (5GY 6/1). All lithologies display color mottling and diagenetic haloes that both obscure and enhance primary features. In places, this produces Liesegang-like laminated bands and haloes of black Mn-oxides(?) (Fig. 5B).

Sediments are slightly to locally heavily bioturbated (including *Zoophycos* trace fossils) and burrows are modified by diagenetic fronts.

In general, sediments are badly fractured and deformed by XCB coring, obscuring many of the finer sedimentary structures. Minor lithologies include vitric ash, occasionally with pumice.

### Depositional Environment

Site 1021 (Gorda Transect, Delgada Fan) is the deepest site (4213 m) drilled during Leg 167. Hence the overall sedimentation rate is low, but fairly constant (30 m/m.y.) since an initially slower rate in the middle Miocene. The sedimentary sequence at this site consists of fine-grained siliciclastic clays with small to large amounts of siliceous and calcareous biogenic components. During the middle to late Miocene, sediments are principally dominated by biosiliceous and calcareous biogenic components, essentially diatoms and calcareous nannofossils, indicating high biogenic productivity, a similar pattern to other deep-water sites on this leg (Sites 1010, 1011, and 1016). According to XRD analysis, however, there is still a significant contribution of siliciclastic material dominated by clay and silt-sized quartz and feldspars. The depositional environment is strongly affected by dissolution of the biogenic component and remains throughout the time interval in the calcite lysocline. From the late Miocene to early Pliocene, the siliciclastic component, essentially clay, increases strongly.

## BIOSTRATIGRAPHY

The sedimentary sequence recovered from the four holes at Site 1021 consists of a well-dated, apparently continuous 310-m-thick interval of uppermost middle Miocene to Quaternary sediments. A well-constrained biostratigraphy and chronology for Hole 1021B is provided by a combination of calcareous nannofossil, planktonic foraminifer, radiolarian, and diatom datums and paleomagnetic reversals. Radiolarians indicate that the base of Hole 1021B is 11.8 Ma in age. An age/depth plot for Hole 1021B (Fig. 6) indicates a remarkably continuous sedimentation rate for the last 10 m.y. Sedimentation rates were lower during the late middle Miocene (~10 to 11.8 Ma; Fig. 6).

Planktonic foraminifers are generally rare to few in number at Site 1021, and most assemblages exhibit evidence of strong calcium carbonate dissolution. During the Quaternary, interglacial assemblages exhibit the strongest effects of dissolution. Benthic foraminifers are rare to absent in most samples. Calcareous nannofossils are generally common and are moderately well preserved. Radiolarian diversity and abundances are high in the Pliocene to middle Miocene sequence, and preservation is generally good. Diatoms are generally common to abundant and moderately to well preserved in the middle and lower upper Miocene and poorly preserved as a result of dissolution from the uppermost Miocene through Quaternary. Diatoms are mostly rare and poorly preserved in the Quaternary, lower Pliocene, and uppermost Miocene.

All of the microfossil groups at Site 1021 are clearly dominated by cool, high-latitude elements from the latest Miocene through the Quaternary. Planktonic foraminifer assemblages are especially representative of cool temperatures during Quaternary glacial episodes and the latest Miocene. Radiolarian assemblages suggest relatively warmer conditions during the middle and early late Miocene.

Radiolarian species characteristic of upwelling environments are scarce throughout most of the sequence, suggesting weak and episodic vertical advection of deep waters at this location. However, both radiolarians and diatoms indicate that upwelling was stronger during the middle through late Miocene and especially strong during the latest Miocene.

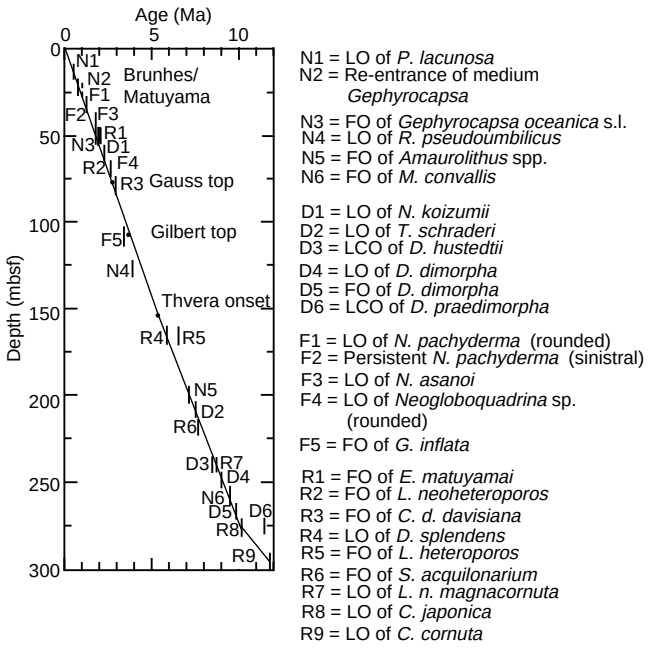


Figure 6. Age/depth plot for Hole 1021B.

Benthic foraminifers indicate that well-oxygenated bottom waters bathed Site 1021 throughout the entire late Neogene.

## Planktonic Foraminifers

Planktonic foraminifers observed in core-catcher samples from Site 1021 range in age from the late Miocene through the Quaternary. The planktonic foraminifer sequence is discontinuous. Most of the core-catcher samples either lack planktonic foraminifers or they are rare to few in number. Most assemblages with foraminifers exhibit strong evidence of calcium carbonate dissolution. During the Quaternary, interglacial assemblages exhibit the strongest effects of dissolution. Benthic foraminifers are rare to absent in most samples and provide the most discontinuous record of all of sites cored during Leg 167. Planktonic foraminifers are common to abundant both during the upper Pliocene from 56 to 103 mbsf (Samples 167-1021B-6H-CC to 11H-CC) and the uppermost Miocene from 185 to 195 mbsf (Samples 167-1021B-20X-CC to 21X-CC).

The planktonic foraminifer sequence of late early Pliocene to Quaternary age at Site 1021 is similar to that of Site 1020. Site 1021 differs from all other sites drilled during Leg 167 in containing planktonic foraminifers of early early Pliocene and late Miocene age, although few assemblages of these ages are preserved because of the intense dissolution in much of this interval. We recognize a sequence of 5 datum levels in the upper Pliocene through Quaternary at Site 1021 as follows: (1) the LO of *Neogloboquadrina pachyderma* (rounded form) at 0.8 Ma (Samples 167-1021B-3H-CC, 167-1021C-4H-CC, and 167-1021D-3H-CC); (2) the FCO of mostly common to abundant populations of sinistral *N. pachyderma* at 1.2 Ma (Samples 167-1021B-3H-CC, 167-1021C-4H-CC, and 167-1021D-3H-CC); (3) the LO of *Neogloboquadrina asanoi* at 1.9 Ma (Samples 167-1021B-6H-CC, 167-1021C-7H-CC, and 167-1021D-7H-CC); (4) the LO of *Neogloboquadrina* sp. (rounded) at 2.25 Ma (Samples 167-1021B-7H-CC); and (5) the FO of *Globorotalia inflata* at 3.3 Ma (Samples 167-1021B-11H-CC, 167-1021C-11H-CC, and 167-1021D-13H-CC) (Table 3).

No datums are recognized below the upper Pliocene because of the discontinuous planktonic foraminifer sequence. Upper Miocene assemblages are marked by the presence of common to abundant sinistral *N. pachyderma*, reflecting especially cool waters during this interval. The FO of *N. pachyderma* occurs at 195 mbsf (Sample 167-1021B-21X-CC). Below the upper Miocene, planktonic foraminifer assemblages have low diversity and are dominated by *Globigerina bulloides.*

Upper Pliocene planktonic foraminifer assemblages at Site 1021 are comprised entirely of cool-temperate to subarctic taxa. Warm-subtropical forms such as *Globigerinoides ruber* are no longer observed even in interglacial assemblages, because of the cooler, higher latitude location of Site 1021. The assemblages are distinctly cool throughout and the diversity within the faunas is generally low. Nevertheless, the assemblages clearly reflect glacial to interglacial oscillations throughout this interval. Early Pliocene assemblages contain rare occurrences of warm subtropical forms reflecting relatively warm-water conditions, the warmest interval inferred for the late Neogene of this site.

Benthic foraminifers in the sequence are typical middle bathyal deep-sea assemblages. The faunas exhibit little change throughout the late Neogene and exhibit no clear oscillations associated with glacial/interglacial change as reflected in the planktonic foraminifer assemblages. Well-oxygenated bottom waters bathed Site 1021 throughout the entire late Neogene.

## Calcareous Nannofossils

Calcareous nannofossils exhibit highly variable preservation and abundance throughout the sequence. Generally they are rare and poorly preserved in the upper and lower Quaternary, lower Pliocene and lower upper Miocene (Table 4). Discoasters in the upper upper Pliocene are rare or absent, because of the cool conditions at this location. Below this interval (~2.6–2.7 Ma), they are few to common. Hole 1021B spans the early late Miocene Zone CN7-CN5b to Pleistocene Zone CN14a. Hole 1021C includes the early Pliocene Zone CN 11 to late Pleistocene Zone CN 15. Hole 1021D spans the early Pliocene Zone CN11 to late Pleistocene Zone CN 15-CN14b. In the Quaternary, calcareous nannofossil assemblages are marked by the presence of *Emiliania huxleyi, Pseudoemiliania lacunosa, Calcidiscus leptoporus, Helicosphaera carteri, H. sellii,* and several morphotypes of *Gephyrocapsa* spp. The Pliocene/Pleistocene boundary is difficult to place because of the near vicinity of barren intervals. Nevertheless, the boundary is placed at the FO of *G. oceanica* s.l. between Sample 167-1021B-4H-CC and 6H-CC in Hole 1021B and at 40.6 mbsf (Sample 167-1021C-5H-CC) in Hole 1021C. Pliocene nannofossil assemblages are marked by an association of *Helicosphaera carteri, H. sellii, Discoaster brouweri, D. tamalis, D. pentaradiatus, D. surculus,* and several morphotypes of *Reticulofenestra.* The lower/upper Pliocene boundary, which is close to the LO of *Reticulofenestra pseudoumbilicus* (base of CN12a), occurs between Samples 167-1021B-12H-CC and 14H-CC in Hole 1021B and at 126.10 mbsf (Sample 167-1021C-13H-CC) in Hole 1021C.

In the upper Miocene, many marker species are absent, making it difficult to develop a precise biostratigraphic assignment of this part of the sequence. However, the presence of *Amaurolithus* spp. in Samples 167-1021C-19X-CC and 21X-CC allows assignment of the upper part of this interval to Zone CN10a-CN9. A few specimens of *Minylitha convallis* indicate the presence of the Zones CN8 and CN9a. The presence of *Discoaster bollii* and *D. exilis,* and the absence of *Minylitha convallis* allows assignment of the base of the sequence to the Zones CN7 through CN5.

## Diatoms

Diatoms are generally common to abundant and moderately to well preserved in the middle and early late Miocene and are poorly preserved as a result of dissolution from the latest Miocene through Quaternary. Assemblages are typical of hemipelagic sedimentary se-

**Table 3. Distribution and relative abundances of planktonic foraminifers in Hole 1021B.**

| Zone | Core, section, interval | Depth (mbsf) | Abundance | Preservation | *Globorotalia inflata* | *Globorotalia scitula* | *Globorotalia crassula* | *Globorotalia decoraperta* | *Globorotalia* cf. *continuosa* | *Globoquadrina altispira altispira* | *Neogloboquadrina asanoi* | *Neogloboquadrina humerosa* | *Neogloboquadrina* n. sp.? | *Neogloboquadrina* sp. "rounded" | *Neogloboquadrina pachyderma* "rounded" | *Neogloboquadrina pachyderma* dex. | *Neogloboquadrina pachyderma* sin. | *Globigerina bulloides* | *Globigerina woodi* | *Globigerina apertura* | *Globigerina quinqueloba* | *Globigerinita glutinata* | *Orbulina universa* | *Globigerinoides ruber* | *Sphaeroidinellopsis paenedehiscens* |
|---|---|---|---|---|---|---|---|---|---|---|---|---|---|---|---|---|---|---|---|---|---|---|---|---|---|
| | 167-1021B- | | | | | | | | | | | | | | | | | | | | | | | | |
| | 1H-CC | 8 | R | M | R | | | | | | | | | | | R | | R | | | | | | | |
| | 2H-CC | 18 | A | M | F | | | | | | | | | | | | A | A | | | | | F | | |
| N22/23 | 3H-CC | 27 | F | M | F | R | | | | | | | | | C | C | C | C | | | | | R | | |
| | 4H-CC | 37 | B | | | | | | | | | | | | | | | | | | | | | | |
| | 5H-CC | 46 | F | P | | | | | | | | F | | | C | | | C | | | | | R | | |
| | 6H-CC | 56 | A | G | | | | | | | A | C | | | | A | A | A | | | C | C | F | | |
| | 7H-CC | 65 | A | M | | | | | | | A | | | C | | A | | A | | | A | | F | | |
| N21 | 8H-CC | 75 | A | G | A | R | | | | | | | | A | | A | | A | | C | A | F | | | |
| | 9H-CC | 84 | F | M | F | | | | | | C | C | | C | | | | | | | | | R | | |
| | 10H-CC | 94 | R | P | A | | | | | | | | | | | | | | | | | | R | | |
| | 11H-CC | 103 | A | G | F | | | | | R | | F | | A | | C | | A | | | | | A | | |
| | 12H-CC | 113 | F | M | | R | R | | | | | C | | | | A | | | | F | | | C | R | |
| N20 | 13H-CC | 122 | R | P | | | | | R | | | | | | | | | F | | | | | F | | |
| | 14H-CC | 132 | B | | | | | | | | | | | | | | | | | | | | | | |
| | 15H-CC | 141 | B | | | | | | | | | | | | | | | | | | | | | | |
| | 16H-CC | 151 | B | | | | | | | | | | | | | | | | | | | | | | |
| N19 | 17H-CC | 160 | R | M | | | | | | | | | F | | | | | F | | | | | F | | |
| | 18H-CC | 170 | B | | | | | | | | | | | | | | | | | | | | | | |
| | 19X-CC | 175 | B | | | | | | | | | | | | | | | | | | | | | | |
| N18 | 20X-CC | 185 | C | G | | | | | | | | | | | | | A | A | F | F | | | F | | |
| | 21X-CC | 195 | C | G | | | | C | | | | | | | | | A | C | C | | | | R | | R |
| | 22X-CC | 204 | B | | | | | | | | | | | | | | | | | | | | | | |
| | 23X-CC | 214 | B | | | | | | | | | | | | | | | | | | | | | | |
| | 24X-CC | 224 | R | M | | R | | | | | | | | | | | | A | | | | | R | | |
| | 25X-CC | 233 | F | G | | | | R | | | | | | | | | | A | C | | R | | R | | |
| | 26X-CC | 243 | B | | | | | | | | | | | | | | | | | | | | | | |
| | 27X-CC | 252 | R | P | | | | | | | | | | | | | | R | | | | | | | |
| N17 | 28X-CC | 262 | B | | | | | | | | | | | | | | | | | | | | | | |
| | 29X-CC | 272 | B | | | | | | | | | | | | | | | | | | | | | | |
| | 30X-CC | 281 | B | | | | | | | | | | | | | | | | | | | | | | |
| | 31X-CC | 291 | B | | | | | | | | | | | | | | | | | | | | | | |
| | 32X-CC | 301 | B | | | | | | | | | | | | | | | | | | | | | | |
| | 33X-CC | 310 | R | M | | | | | | | | | | | | | | F | | | | | | | |

Note: See "Explanatory Notes" chapter for abbreviations.

quences of temperate middle latitudes, and the standard North Pacific diatom zonation has been adapted for use at Hole 1021B (Table 5). Reworked forms and neritic assemblages are not important at this site. Sparse occurrences of subtropical taxa including *Actinocyclus ellipticus, Azpeitia nodulifer, Crucidenticula nicobarica, C. punctata,* and *Hemidiscus cuneiformis* may indicate the influence of warmer waters.

A poorly preserved interval from 55.5 to 84.0 mbsf is generally correlative with the late Pliocene zones from the *Neodenticula koizumii* Zone (NPD 9) to the underlying *N. koizumii-Neodenticula kamtschatica* Zone (NPD 8), based on the presence of consistent *N. koizumii* and *Thalassiosira convexa.* Sample 167-1021-15H-CC (141 mbsf) is assigned to subzone interval b–c of the *N. kamtschatica* Zone (NPD 7), based on the presence of rare *N. kamtschatica* and *Thalassiosira oestrupii.*

Characteristic lower Pliocene subarctic assemblages dominated by *N. kamtschatica* and *Coscinodiscus marginatus* are missing at Site 1021 because of the warm-temperate conditions. Thus, it is inferred that an unzoned interval between Samples 167-1021B-16H-CC and 22X-CC is equivalent in age to Subzone interval a of the *N. kamtschatica* Zone (NPD 7).

A complete sequence of diatom zones from the late Miocene *Thalassionema schraderi* Zone (NPD 6b) to the middle Miocene *Denticulopsis praedimorpha* Zone (NPD 5b) was penetrated in the lower half part (>214 mbsf) of Hole 1021B. Assemblages in Samples 167-1021-27X-CC and 28X-CC (252.4 to 262.1 mbsf) containing *Denticulopsis dimorpha* are assigned to the early late Miocene *D. dimorpha* Zone (NPD 5d). The consistent occurrence of *D. praedimorpha* in Samples 167-1021B-30X-CC through 33X-CC corresponds to the *D. praedimorpha* Zone (NPD 5b) and indicates that the base of Hole 1021B is younger than 12.8 Ma.

Specimens of *Thalassiothrix,* including *T. longissima,* are especially abundant and of large size in late to middle Miocene assemblages, indicating high oceanic productivity during this time. In contrast, specimens of *Denticulopsis* are mainly represented by small size compared with those in diatom assemblages from the northwest Pacific.

## Radiolarians

Quaternary sediments are barren of radiolarians at Site 1021. Radiolarian diversity is very high in the Pliocene to middle Miocene se-

**Table 4. Distribution and relative abundances of calcareous nannofossils in Holes 1021A, 1021B, 1021C, and 1021D.**

| Zone | Core, section, interval | Depth (mbsf) | Preservation | Abundance | *Emiliania huxleyi* | *Pseudoemiliania lacunosa* | *Helicosphaera carteri* | *Helicosphaera sellii* | *Gephyrocapsa oceanica* s.l. | *Gephyrocapsa* sp. 3 | *Gephyrocapsa* small | *Discoaster brouweri* | *Discoaster pentaradiatus* | *Discoaster surculus* | *Discoaster tamalis* | *Discoaster asymmetricus* | *Sphenolithus* spp. | *Reticulofenestra pseudoumbilicus* | *Ceratholithus* spp. | *Amaurolithus* spp. | *Minylitha convallis* | *Coccolithus pelagicus* | *Calcidiscus macintyrei* >11 µm | *Calcidiscus leptoporus* | *Discoaster exilis* | *Discoaster bollii* |
|---|---|---|---|---|---|---|---|---|---|---|---|---|---|---|---|---|---|---|---|---|---|---|---|---|---|---|
| CN15–CN14b | 167-1021A-<br>1H-CC | 9.90 | M | F/C | | | | | P | | C | | | | | | | | | | | R | | | | |
| | 167-1021B- | | | | | | | | | | | | | | | | | | | | | | | | | |
| | 1H-CC | 8.00 | | B | | | | | | | | | | | | | | | | | | | | | | |
| | 2H-6, 23 | 15.73 | | B | | | | | | | | | | | | | | | | | | | | | | |
| CN14a | 2H-7, 23 | 17.23 | G | A | | C | | | C | | A | | | | | | | | | | | | | P | | |
| CN14a | 2H-CC | 17.50 | G | A | | F/C | R | | R/F | | A | | | | | | | | | | | F | | | | |
| CN14a | 3H-1, 22 | 20.72 | G | C/A | | R | | | C | | A | | | | | | | | | | | F | | R | | |
| CN14a–CN13b | 3H-CC | 27.00 | P/M | F | | C | | | | | P | | | | | | | | | | | | | C | | |
| | 4H-6, 23 | 31.73 | | B | | | | | | | | | | | | | | | | | | | | | | |
| CN13b? | 4H-CC | 36.50 | P | RR | | | | | | | R | | | | | | | | | | | | | | | |
| | 5H-1, 46 | 36.96 | | B | | | | | | | | | | | | | | | | | | | | | | |
| | 5H-4, 23 | 41.23 | | B | | | | | | | | | | | | | | | | | | | | | | |
| | 5H-6, 23 | 44.23 | | B | | | | | | | | | | | | | | | | | | | | | | |
| | 5H-7, 23 | 45.73 | | B | | | | | | | | | | | | | | | | | | | | | | |
| | 5H-CC | 46.00 | | B | | | | | | | | | | | | | | | | | | | | | | |
| CN13a–CN12 | 6H-CC | 55.50 | P/M | C/A | | P | R | R | | | | | | | | | | | | | | | R | C | | |
| | 7H-7, 23 | 64.73 | | B | | | | | | | | | | | | | | | | | | | | | | |
| CN13a–CN12 | 7H-CC | 65.00 | M | A | | C | | | | | | | | | | | | | | | | F | | F/C | | |
| CN13a–CN12 | 8H-CC | 74.50 | P/M | F/C | | P | | | | | | | | | | | | | | | | R | | C | | |
| | 9H-CC | 84.00 | | B | | | | | | | | | | | | | | | | | | | | | | |
| CN12a | 10H-CC | 93.50 | G | A | | P | | | | | | | P | P | F/C | R | | | | | | | C | R | | |
| CN12a | 11H-CC | 103.00 | G | A | | | | | | | | R | F | F | F | | | | | | | F | C | C | | |
| CN12a | 12H-CC | 112.50 | M/G | C | | R | | | | | | R | | F | | | | | | | | | | F/C | | |
| | 13H-CC | 122.00 | | B | | | | | | | | | | | | | | | | | | | | | | |
| CN11 | 14H-CC | 131.50 | P | F | | | | | | | | | | | | | | F/R | | | | F | | F | | |
| CN11? | 15H-CC | 141.00 | P | R | | | | | | | | | | | | | | R | | | | | | R | | |
| CN11? | 16H-CC | 150.50 | P | R | | | | | | | | | R | R | | | | | | | | R | | R | | |
| | 17H-CC | 160.00 | P | F | | | | | | | | | R | | | | | F | | | | | | | | |
| | 18H-CC | 169.50 | P | R | | | | | | | | | | | | | | R | | | | | | | | |
| CN10a–CN9 | 19X-CC | 175.40 | M | A | | | R | | | | | P | F/C | | | | P | C | | R | | R | | | | |
| CN10a–CN9 | 20X-CC | 185.00 | P/M | C/A | | | R | | | | | | R | | | | P | C | | | | | P | R | | |
| CN10a–CN9 | 21X-CC | 194.70 | M | A | | | | | | | | | | | | | | C | | R | | | R | | | |
| | 22X-CC | 204.30 | | B | | | | | | | | | | | | | | | | | | | | | | |
| | 23X-CC | 214.00 | | B | | | | | | | | | | | | | | | | | | | | | | |
| CN9a–CN8 | 24X-CC | 223.60 | M | A | | | | | | | | | | | | | | C | | | R/F | F | | R | | |
| CN9a–CN8 | 25X-CC | 233.20 | M | F/C | | | | | | | | | | | | | | P | | | R | | | | | |
| CN9a–CN8 | 26X-CC | 242.80 | P | R | | | | | | | | | | | | | | R | | | RR | | | | | |
| CN9a–CN8 | 27X-CC | 252.40 | M | A | | | | | | | | | | | | | | C | | | F | P | | | | |
| | 28X-CC | 262.10 | | B | | | | | | | | | | | | | | | | | | | | | | |
| CN7–CN5b | 29X-CC | 271.70 | M | A | | | | | | | | | | | | | R | C/A | | | | | | | P | |
| | 30X-CC | 281.30 | | B | | | | | | | | | | | | | | | | | | | | | | |
| | 31X-CC | 290.90 | | B | | | | | | | | | | | | | | | | | | | | | | |
| CN7–CN5b | 32X-CC | 300.50 | P | F | | | | | | | | | | | | | | P | | | | | | | P | P |
| CN7–CN5b | 33X-CC | 310.20 | P | R | | | | | | | | | | | | | | P | | | | | | | P | P |
| | 167-1021C- | | | | | | | | | | | | | | | | | | | | | | | | | |
| CN15 | 1H-CC | 2.60 | M | F/C | P | | | | C | | P | | | | | | | | | | | | | | | |
| CN15–CN14b | 2H-CC | 12.10 | P | R | | | | | RR | RR | R | | | | | | | | | | | P | | F | | |
| | 3H-CC | 21.60 | | B | | | | | | | | | | | | | | | | | | | | | | |
| CN14a | 4H-CC | 31.10 | P | RR | | RR | | | | | | | | | | | | | | | | | | | | |
| CN13b | 5H-CC | 40.60 | P | R | | R | | | R | | R | | | | | | | | | | | | | R | | |
| CN13a | 6H-CC | 50.10 | M | C | | C | R | R | | | | | | | | | | | | | | R | | F/C | | |
| CN13a–CN12 | 7H-CC | 59.60 | P | C | | C | | | | | | | | | | | | | | | | R | R | C | | |
| CN13a–CN12 | 8H-CC | 69.10 | P | RR | | | | | | | P | | | | | | | | | | | P | | | | |
| CN12 | 9H-CC | 78.60 | P | R/F | | R | | | | | | R | | R | | | | | | | | | | | | |
| CN12 | 10H-CC | 88.10 | G | A | | R | | | | | | R | F | C | | | | | | | | F | | R | | |
| CN12 | 11H-CC | 97.60 | G | A | | P | | | | | | | P | F | | | | | | | | F | R | F | | |
| CN12? | 12H-CC | 107.10 | P | RR | | R | | | | | | | | | | | | | | | | | | | | |
| CN12? | 13H-CC | 116.60 | P | F/C | | | | | | | | | | F | | | | RR | | RR | | R | F/R | F | | |
| CN11 | 14H-CC | 126.10 | M/G | A | | | | | | | | | C | | | | P | C | | RR | | P | C | | | |
| | 15H-CC | 135.60 | | B | | | | | | | | | | | | | | | | | | | | | | |
| CN11? | 16H-CC | 145.10 | P | R | | | | | | | | P | R | | | | | | | | | | R | | | |
| | 17H-CC | 154.60 | P | RR | | | | | | | | | | | | | | | | | | R | R | | | |
| | 18H-CC | 164.10 | P | RR | | | | | | | | | | | | | | R | | | | | | | | |
| | 167-1021D- | | | | | | | | | | | | | | | | | | | | | | | | | |
| CN15–CN14b | 1H-CC | 5.50 | P | R | | | | | | | R | | | | | | | | | | | F | | | | |
| CN14a | 2H-CC | 15.00 | G | A | | F | | | F | | A | | | | | | | | | | | | | R | | |
| CN14a–CN13b | 3H-CC | 24.50 | P | R | | | | | | | P | | | | | | | | | | | | | | | |
| | 4H-CC | 34.00 | | B | | | | | | | | | | | | | | | | | | | | | | |
| CN13b | 5H-CC | 43.50 | P | RR | | R | | | R | | | | | | | | | | | | | R | | | | |
| | 6H-CC | 53.00 | P | RR | | R | | | | | | | | | | | | | | | | | | | | |
| CN13a–CN12 | 7H-CC | 62.50 | M/G | A | | C | | | | | | | | | | | | | | | | F | R | C | | |
| CN13a–CN12 | 8H-CC | 72.00 | P | R | | R | | | | | | | | | | | | | | | | R | | R | | |

**Table 4 (continued).**

| Zone | Core, section, interval | Depth (mbsf) | Preservation | Abundance | *Emiliania huxleyi* | *Pseudoemiliania lacunosa* | *Helicosphaera carteri* | *Helicosphaera sellii* | *Gephyrocapsa oceanica* s.l. | *Gephyrocapsa* sp. 3 | *Gephyrocapsa* small | *Discoaster brouweri* | *Discoaster pentaradiatus* | *Discoaster surculus* | *Discoaster tamalis* | *Discoaster asymmetricus* | *Sphenolithus* spp. | *Reticulofenestra pseudoumbilicus* | *Ceratholithus* spp. | *Amaurolithus* spp. | *Minylitha convallis* | *Coccolithus pelagicus* | *Calcidiscus macintyrei* >11 µm | *Calcidiscus leptoporus* | *Discoaster exilis* | *Discoaster bollii* |
|---|---|---|---|---|---|---|---|---|---|---|---|---|---|---|---|---|---|---|---|---|---|---|---|---|---|---|
| CN12 | 9H-CC | 81.50 | M | C | | P | | | | | | R | R | | | | | | | | | C | | R | | |
| CN12 | 10H-CC | 91.00 | G | A | | R | | | | | | R | F | P | R | | | | R | | | | F/C | C | | |
| CN12 | 11H-CC | 100.50 | G | A | | C | | | | | | | R | F | | | | | | | | F | C | P | | |
| | 12H-CC | 110.00 | | B | | | | | | | | | | | | | | | | | | | | | | |
| CN12 | 13H-CC | 119.50 | G | C/A | | R | | R | | | | | R | | | | | | | | | F | C/F | P | | |
| | 14H-CC | 129.00 | | B | | | | | | | | | | | | | | | | | | | | | | |
| CN11? | 15H-CC | 138.50 | P | R | | | | | | | | | | | | | | R | | | | | | | | |

Note: See "Explanatory Notes" chapter for abbreviations.

quence and preservation is generally good. A total diversity of 64 species was tabulated for the core-catcher samples of Hole 1021B (Table 6). The main radiolarian events are tabulated for Holes 1021B and 1021C (Table 7). The occurrence of subtropical and temperate radiolarian species such as *Cyrtocapsella cornuta, Theocorys redondoensis,* and *Stichocorys armata* provides an age of 11.8 Ma for the base of the cored sequence. The Pliocene/Pleistocene and Miocene/Pliocene boundaries cannot be placed because of barren or poor assemblages in key intervals. The middle/late Miocene boundary is located at the LO of *Cyrtocapsella japonica* between Samples 167-1021B-31X-CC (290.9 mbsf) and 32X-CC (300.5 mbsf).

Nine major radiolarian events are recognized in Hole 1021B (Table 7). All of them, except for the FO of *Lamprocyrtis heteroporos,* are perfectly intercalibrated with, and contribute to, the magnetobiostratigraphic scheme for Site 1021 (Fig. 6). A number of radiolarian events, such as the LO of *Stichocorys peregrina,* were not employed because of known strong diachronism.

Subarctic species are dominant in upper Miocene to upper Pliocene assemblages. Lower upper Miocene and middle Miocene assemblages contain temperate or subtropical forms. Radiolarian species characteristic of upwelling environments are scarce throughout most of the sequence, suggesting weak and episodic vertical advection of deep waters at this location. However, upwelling was distinctly stronger during the late Miocene.

## PALEOMAGNETISM

We made magnetic measurements with the pass-through cryogenic magnetometer on the archive halves of 18 APC cores from Hole 1021B. After measuring the natural remanent magnetization (NRM), the sections were demagnetized with a peak alternating field (AF) of 20 mT. At Hole 1021C, the archive halves of the 18 APC cores were measured after demagnetization at 20 mT without NRM measurement. At both holes the intensity of remanent magnetization after AF demagnetization is about 20 mA/m for the top 40 mbsf (Figs. 7, 8). The intensity of the NRM is about 100 mA/m in this interval. Between 40 and 55 mbsf there is an approximately 40-fold decrease in the intensity of magnetization. The intensity of NRM before and after demagnetization does not vary much with depth between 55 and 170 mbsf. A similar depth dependence was observed for the magnetic susceptibility of these cores (see "Physical Properties" section, this chapter). There is a smaller decrease in magnetization after AF demagnetization in the top 40 mbsf of Hole 1021B than in the lower part. The difference in intensity decrease could be caused by finer and higher coercivity magnetic grains in the upper part of the hole as opposed to larger and lower coercivity grains in the lower part of the hole. Dissolution of the smallest magnetic particles below 40 mbsf might be a possible explanation.

The polarity chrons in Figures 7 and 8 were determined based on the inclinations. The correlation to the standard time scale (Cande and Kent, 1995) was straightforward. Nearly all reversal boundaries between Chron C1n (Brunhes) and the onset of Subchron C3n.4n (Thvera) at 5.23 Ma could be identified in the magnetostratigraphic records of Hole 1021B and 1021C (Tables 8, 9). The positive inclinations around 32 mbsf in Hole 1021B (Fig. 7) probably represent Subchron C1r.1n (Jaramillo), but the transition boundaries are not clearly resolved because of a drilling-induced magnetic overprint. Fortunately, the inclination record of Hole 1021C complements the record of Hole 1021B, and the Jaramillo subchronozone boundaries could be determined there. The onset of Subchron C3n.3n (Sidufjall) and the termination of Subchron C3n.4n (Thvera) could not be precisely determined at either Holes 1021B or 1021C, and they were not assigned ages in Figures 7 and 8. The depth range over which each reversal occurs is quite well constrained, as expressed by the small difference between the upper and lower limit for each reversal (Tables 8, 9).

A plot of the ages of the magnetic reversals vs. the sub-bottom depth (Fig. 9) reveals a constant sedimentation rate of 30 m/m.y. throughout the Pliocene and Pleistocene in both holes. Considering the uncertainty limits in the reversal boundaries (open and closed triangles in Fig. 9), the transitions occur virtually at the same depths at both holes. This section will serve as a well-dated reference for the calibration of biostratigraphic datums.

After orienting the APC cores with the Tensor tool, the corrected declinations of Cores 167-1021B-3H to 11H and Cores 167-1021C-3H to 12H (open circles in Figs. 7, 8) scatter around 0° in the normal polarity zones and around 180° in the reversed polarity intervals. In most parts of the holes, the declination data support the interpretation of magnetic polarity zonation based on the inclination data. Possible sources for the deviation of the declinations from the expected values could be the core-splitting procedure, experimental error in the Tensor tool measurement, or insufficient removal of a drilling overprint. In summary, the inclination data were of very good quality and sufficient to determine the >5-m.y.-long magnetostratigraphy at Site 1021.

## COMPOSITE DEPTHS AND SEDIMENTATION RATES

Multisensor track (MST) data collected at 4-cm intervals from Holes 1021A through 1021D and color reflectance data collected at 6-cm intervals from Holes 1021B and 1021C were used to determine

**Table 5. Distribution and relative abundances of diatoms in Holes 1021A and 1021B.**

| Geologic age | North Pacific diatom zone | Numeric age (Ma) | Core, section, interval | Sample depth (mbsf) | Abundance | Preservation | Comments | *Actinocyclus ellipticus javanica* | *Actinocyclus ingens* | *Actinocyclus oculatus* | *Actinocyclus* cf. *oculatus* | *Actinocyclus tsugaruensis* | *Actinoptychus senarius* | *Azpeitia nodulifer* | *Cocconeis costata* | *Coscinodiscus marginatus* | *Coscinodiscus marginatus fossilis* | *Coscinodiscus radiatus* | *Crucidenticula nicobarica* | *Crucidentucla punctata* | *Denticulopsis dimorpha* | *Denticulopsis* cf. *dimorpha* | *Denticulopsis hustedtii* | *Denticulopsis hustedtii* (elliptical) | *Denticulopsis katayamae* | *Denticulopsis* cf. *katayamae* | *Denticulopsis lauta* s.l. | *Denticulopsis praedimorpha* | *Hemiaulus polymorphus* | *Hemidiscus cuneiformis* | *Neodenticula kamtschatica* | *Neodenticula koizumii* | *Neodenticula* cf. *koizumii* |
|---|---|---|---|---|---|---|---|---|---|---|---|---|---|---|---|---|---|---|---|---|---|---|---|---|---|---|---|---|---|---|---|---|
| ? | Unzoned | | 167-1021A-<br>1H-CC | 9.9 | B | | Clay | | | | | | | | | | | | | | | | | | | | | | | | | |
| | | | 167-1021B- | | | | | | | | | | | | | | | | | | | | | | | | | | | | | |
| | | | 1H-CC | 8.0 | B | | Clay | | | | | | | | | | | | | | | | | | | | | | | | | |
| | | | 2H-CC | 17.5 | B | | Clay | | | | | | | | | | | | | | | | | | | | | | | | | |
| ? | Unzoned | | 3H-CC | 27.0 | B | | Clay | | | | | | | | | | | | | | | | | | | | | | | | | |
| | | | 4H-CC | 36.5 | B | | Clay | | | | | | | | | | | | | | | | | | | | | | | | | |
| | | | 5H-CC | 46.0 | T | P | Clay | | | | T | | | | | | | | | | | | | | | | | | | | | |
| | | 2.0? | 6H-CC | 55.5 | A | P/M | Diatomaceous | | | T | | | | | T | F | | | | | | | | | | | | | F | | F | |
| late Pliocene | | | 7H-CC | 65.0 | F | P | Clay | | | | | | | | | | | | | | | | | | | | | | | | F | |
| | NPD 9–NPD 8 | | 8H-CC | 74.5 | C | P/M | Dissolution | | | R | | | | | | R | | | | | | | | | | | | | | F | |
| | | | 9H-CC | 84.0 | R | P | Dissolution | | | | | | | | | R | | | | | | | | | | | | | | | | T |
| | | 3.51? | 10H-CC | 93.5 | T | P | Clay + nannofossils | | | | | | | | | | | | | | | | T | | | | | | | | | |
| | | | 11H-CC | 103.0 | T | P | Clay + nannofossils | | | | | | | | | T | | | | | | | | | | | | | | | | |
| early Pliocene? | Unzoned | | 12H-CC | 112.5 | R | P | Clay + dissolution | | | | | | | | | | | | | | | | T | | | | | | | | | |
| | | | 13H-CC | 122.0 | T | P | Clay + dissolution | | | | | | | | | | | | | | | | T | | | | | | | | | |
| | | | 14H-CC | 131.5 | T | P | Clay + dissolution | | | | | | | | | | | | | | | | | | | | | | | | | |
| | NPD 7c–7b | | 15H-CC | 141.0 | A | P | Clay + upwelling | | | | | | | | | C | | | | | | | | | | | | | R | R | | |
| | | 5.3? | 16H-CC | 150.5 | R | P | Clay + dissolution | | | | | | | | | R | | | | | | | | | | | | | | | | |
| | | | 17H-CC | 160.0 | F | P | | | | | | | T | | | | | | | | | | | | | | | | | | | |
| | | | 18H-CC | 169.5 | A | P | Clay + upwelling? | | | | | | | A | | C | | | | | | | T | | | | | | | | | |
| late Miocene? | Unzoned | | 19X-CC | 175.4 | F | P | Clay + dissolution | | | | | | | | | | | | | | | | T | | | | | | | | | |
| | | | 20X-CC | 185.0 | A | P | Clay | | | | | | | | | | | | | | | | T | | | | | | T | | | |
| | | | 21X-CC | 194.7 | T | P | Clay | | | | | | | | | T | | | | | | | | | | | | | | | | |
| | | | 22X-CC | 204.3 | R | P | | | | | | | | | | T | | | | | | | | | | | | | | | | |
| | | 7.4 | 23X-CC | 214.0 | A | P | Upwelling | | | | | | | | | C | | | | | | T | | | | | T | | | | | |
| | NPD 6b | | 24X-CC | 223.6 | A | P/M | Upwelling | | | | | | | | | R | | | | | | R | | | | | | | | T | | |
| late Miocene | | 8.4 | 25X-CC | 233.2 | A | P | Upwelling | | | | | R | | | | R | R | R | | | | | | | | R | R | | | | | |
| | NPD 6a | | 26X-CC | 242.8 | A | P/M | Diatomite | | | | | | R | F | | F | R | | | | | R | F | | | R | | | | R | | |
| | | 9.0 | 27X-CC | 252.4 | A | M/G | Diatomite | | F | | | | | | | | | | T | | R | | C | R | R | | | T | | R | | |
| | NPD 5d | | 28X-CC | 262.1 | A | M | Diatomite | R | R | | | F | | | | | | | | | F | | | | | | | | | | | |
| | NPD 5c | 9.8 | 29X-CC | 271.7 | A | P/M | Dissolution | R | F | | | R | | | | R | | | | | | | R | | | | | | | | | |
| | | 11.4 | 30X-CC | 281.3 | C | P/M | Dissolution | | F | | | | | | | T | | | | | | | F | | | | | R | | | | |
| middle Miocene | NPD 5b | | 31X-CC | 290.9 | C | P/M | Diatomaceous | | F | | | | | R | | R | | | | | | | F | | | | | F | F | | | |
| | | | 32X-CC | 300.5 | A | M | Dissolution, warm | | C | | | | | | | | | | | F | | | C | | | | | F | | | | |
| | | <12.8 | 33X-CC | 310.2 | A | M/G | Upwelling, dissolution | | F | | | | | | | F | | | | | | | C | | | | | C | | | | |

Note: See “Explanatory Notes” chapter for abbreviations.

**Table 5 (continued).**

| Geologic age | North Pacific diatom zone | Numeric age (Ma) | Core, section, interval | Sample depth (mbsf) | Abundance | Preservation | Comments | *Neodenticula seminae* | *Neodenticula seminae* (sensu Akiba) | *Nitzschia fossilis* | *Nitzschia porteri* | *Nitzschia reinholdii* | *Nitzschia rolandii* | *Nitzschia* sp. | *Paralia sulcata* | *Rhizosolenia barboi* | *Rhizosolenia* sp. | *Rouxia californica* | *Stephanopyxis turris* | *Thalassionema hirosakiensis* | *Thalassionema nitzschioides* | *Thalassionema nitzschioides parva* | *Thalassionema robusta* | *Thalassionema schraderi* | *Thalassiosira antiqua* | *Thalassiosira convexa* | *Thalassiosira* cf. *convexa* | *Thalassiosira leptopus* | *Thalassiosira oestrupii* | *Thalassiothrix longissima* | *Thalassiothrix* spp. | Diatom fragments | Diatom fragments (girdle bands) |
|---|---|---|---|---|---|---|---|---|---|---|---|---|---|---|---|---|---|---|---|---|---|---|---|---|---|---|---|---|---|---|---|---|
| ? | Unzoned | | 167-1021A-<br>1H-CC | 9.9 | B | | Clay | | | | | | | | | | | | | | | | | | | | | | | | | |
| | | | 167-1021B-<br>1H-CC | 8.0 | B | | Clay | | | | | | | | | | | | | | | | | | | | | | | | | |
| | | | 2H-CC | 17.5 | B | | Clay | | | | | | | | | | | | | | | | | | | | | | | | | |
| ? | Unzoned | | 3H-CC | 27.0 | B | | Clay | | | | | | | | | | | | | | | | | | | | | | | | T | |
| | | | 4H-CC | 36.5 | B | | Clay | | | | | | | | | | | | | | | | | | | | | | | | | |
| | | | 5H-CC | 46.0 | T | P | Clay | R | | | | | | | T | | | | | | | | | | | | | | | | |
| | | 2.0? | 6H-CC | 55.5 | A | P/M | Diatomaceous | T | R | | | F | | | | F | | | R | | | | | | | | | T | F | C | | |
| late Pliocene | | | 7H-CC | 65.0 | F | P | Clay | | | | | | | | | F | | | R | | | | | | | | T | | | | | |
| | NPD 9–NPD 8 | | 8H-CC | 74.5 | C | P/M | Dissolution | | R | | | R | | | | C | | | C | | R | | T | | T | | | | R | F | | |
| | | | 9H-CC | 84.0 | R | P | Dissolution | | | | | | | | | T | | | T | | | | | | | T | | | | | | |
| | | 3.51? | 10H-CC | 93.5 | T | P | Clay + nannofossils | | | | | | | | | T | | | | | | | | | | | | | | | | T |
| | | | 11H-CC | 103.0 | T | P | Clay + nannofossils | | | | | | | | | | | | T | | | | | | | | | | | | T | R |
| early Pliocene? | Unzoned | | 12H-CC | 112.5 | R | P | Clay + dissolution | | | | | | | | | F | T | | R | | | | | | | | | | T | | | |
| | | | 13H-CC | 122.0 | T | P | Clay + dissolution | | | | | | | | | R | | | T | | T | | | | | | | | | | | |
| | | | 14H-CC | 131.5 | T | P | Clay + dissolution | | | | | | | | | R | | | T | | | | | | | | | | | | | |
| | NPD 7c–7b | | 15H-CC | 141.0 | A | P | Clay + upwelling | | | | | T | T | | | C | | | R | | C | | | | | | | | T | C | A | | |
| | | 5.3? | 16H-CC | 150.5 | R | P | Clay + dissolution | | | | | | | | | R | | | | | R | | R | | | | | | | | | |
| | | | 17H-CC | 160.0 | F | P | | | | | T | | | | | | | | | | | | | | T | | | T | | | R | |
| | | | 18H-CC | 169.5 | A | P | Clay + upwelling? | | | | T | | T | | | | | | | | | | | | | | | | T | | | | |
| late Miocene? | Unzoned | | 19X-CC | 175.4 | F | P | Clay + dissolution | | | | | | | | T | | | | | | T | | | | | | | | R | | | |
| | | | 20X-CC | 185.0 | A | P | Clay | | | T | | | | | | | | | T | | R | | | | | | | | | A | | A |
| | | | 21X-CC | 194.7 | T | P | Clay | | | | | | | | | | T | | | | T | | | | | | | | | | | T |
| | | | 22X-CC | 204.3 | R | P | | | | | | | | | | | | | | | | | | | | | | | | | C | R |
| | | 7.4 | 23X-CC | 214.0 | A | P | Upwelling | | | | | | | | | R | | | | | | | | T | | | | | | A | | |
| | NPD 6b | | 24X-CC | 223.6 | A | P/M | Upwelling | | | | | | | R | | R | | | T | | | | | F | | | | | C | A | | |
| late Miocene | | 8.4 | 25X-CC | 233.2 | A | P | Upwelling | | | R | | | | | | F | | F | R | | R | | | | | | | | | A | | |
| | NPD 6a | | 26X-CC | 242.8 | A | P/M | Diatomite | | | | | | | | | | | | | | | | | | | | | | | R | | |
| | | 9.0 | 27X-CC | 252.4 | A | M/G | Diatomite | | | | | | | | | F | | | | | | | | | | | | | | | A | |
| | NPD 5d | | 28X-CC | 262.1 | A | M | Diatomite | | | | | | | | | R | | | | | | | | | | | | | | C | A | |
| | NPD 5c | 9.8 | 29X-CC | 271.7 | A | P/M | Dissolution | | | | | | | | | | | | | | | | | | | | | | | R | | |
| | | 11.4 | 30X-CC | 281.3 | C | P/M | Dissolution | | | | | | | | | | | | | | | | T | | | | | | | R | | |
| middle Miocene | NPD 5b | | 31X-CC | 290.9 | C | P/M | Diatomaceous | | | | | | | | | | | | | R | F | | | | | | | | | | | |
| | | | 32X-CC | 300.5 | A | M | Dissolution, warm | | | | | | | | | | | | | | | | | | | | | | | F | | |
| | | <12.8 | 33X-CC | 310.2 | A | M/G | Upwelling, dissolution | | | | | | | | | | | | | | | | | | | | | | | A | A | |

**Table 6. Distribution and relative abundance of radiolarians in Hole 1021B.**

| Zone | Core, section, interval | Depth (mbsf) | Abundance | Preservation | *Stichocorys armata* | *Gondwanaria hister* gr. | *Theocorys redondoensis* | *Amphymenium amphistylium* | *Prunopyle hayesi* | *Lychnocanoma nipponica nipponica* | *Siphocampe modeloensis* | *Stichocorys delmontensis* | *Phormostichoartus fistula* | *Cyrtocapsella cornuta* | *Cyrtocapsella japonica* | *Diartus pettersoni* | *Lychnocanoma nipponica magnacornuta* | *Tricolospyris leibnitziana* | *Stauroxiphos communis* | *Dictyophimus splendens* | *Cycladophora cosma* | *Anthocyrtidium pliocenica* | *Stylatractus universus* | *Lithopera neotera* | *Eucyrtidium acuminatum* | *Stylodictya validispina* | *Prunopyle tripopyrena* | *Botryostrobus bramlettei* | *Larcospira moschkovskii* | *Dendrospyris bursa* | *Eucyrtidium teuscheri* | *Lamprocyclas hannai* | *Diartus hughesi* | *Didymocyrtis laticonus* | *Rhizosphaera antarctica* | *Anthocyrtella? callopisma* | *Stichocorys peregrina* | *Stichocorys radicula* |
|---|---|---|---|---|---|---|---|---|---|---|---|---|---|---|---|---|---|---|---|---|---|---|---|---|---|---|---|---|---|---|---|---|---|---|---|---|---|
| Unzoned | 167-1021B- | | | | | | | | | | | | | | | | | | | | | | | | | | | | | | | | | | | | |
| | 1H-CC | 8.0 | B | | | | | | | | | | | | | | | | | | | | | | | | | | | | | | | | | | |
| | 2H-CC | 17.5 | B | | | | | | | | | | | | | | | | | | | | | | | | | | | | | | | | | | |
| | 3H-CC | 27.0 | R | P | | | | | | | | | | | | | | | | | | | | | | | | | | | | | | | | | |
| | 4H-CC | 36.5 | B | | | | | | | | | | | | | | | | | | | | | | | | | | | | | | | | | | |
| *E. matuyamai* | 5H-CC | 46.0 | R | P | | | | | | | | | | | | | | | | | | | R | | | | | | | | | | | | | | |
| *S. langii* | 6H-CC | 55.5 | A | G | | | | | | | | | | | | | | | | | | | C | | F | | | | | R | | | | R | | | |
| | 7H-CC | 65.0 | A | M | | | | | | | | | | | | | | | | | | | F | | R | F | | | | R | | | | R | | | |
| | 8H-CC | 65.0 | C | M | | | | | | | | | | | | | | | | | | | F | | R | | | | | R | | | | | T | | |
| | 9H-CC | 84.0 | F | G | | | | | | | | | | | | | | | | | | | R | | R | | | | | | | | | | | | |
| | 10H-CC | 93.5 | R | G | | | | | | | | | | | | | | | | | | | | | | | | | | | | | | | | | |
| | 11H-CC | 103.0 | R | G | | | | | | | | | | | | | | | | | | | | | | | | | | | | | | | | | |
| | 12H-CC | 112.5 | R | G | | | | | | | | | | | | | | | | | | | P | | | P | | | | | | | | P | | | |
| *S. peregrina* | 13H-CC | 122.0 | R | G | | | | | | | | | | | | | | | | | | | P | | | P | P | | | | | | | P | | | |
| | 14H-CC | 131.0 | R | M | | | | | | | | | | | | | | | | | | | P | | | | | | | | | | | | | P | |
| | 15H-CC | 141.0 | A | G | | | | | | | T | T | R | | | | | | | | | R | C | | T | | | | | | | R | | | | F | |
| | 16H-CC | 150.5 | C | G | | | | | | | | | | | | | | | | | T | | F | | T | R | T | | | | | | | R | | R | |
| | 17H-CC | 160.0 | C | G | | | | | | | | | | | | | | | | | | | C | | | R | R | | | | | | | R | R | T | |
| | 18H-CC | 169.5 | A | G | | | | | | | | | | | | | | | | T | | F | C | | R | R | | | T | | | R | | | R | A | |
| | 19X-CC | 175.4 | F | G | | | | | | | T | | | | | | | | | R | | | C | | R | | | | | | | R | | | R | A | |
| | 20X-CC | 185.0 | C | G | | | | | R | T | | | | | | | | | | C | | | C | | | C | | R | R | | R | R | | | R | C | |
| | 21X-CC | 194.7 | R | M | | | | | | | | | | | | | | | | | | | T | | | T | | | | | | | | | | T | |
| | 22X-CC | 204.3 | F | G | | | | T | T | | R | R | | | | | | | | C | | R | C | R | R | C | | T | | | T | T | | | | A | |
| | 23X-CC | 214.0 | A | G | | | R | | | R | | C | | | | | | | R | R | | | R | | | F | | | | | | | | R | | A | |
| *D. penultima* | 24X-CC | 223.6 | C | G | | | | T | | F | | A | | | | | | | | F | T | R | | | | | | | | | R | | | | R | | | |
| | 25X-CC | 233.2 | A | G | | | | | R | R | | A | | | | | | T | | A | R | C | C | | T | R | | A | | R | | | | R | R | R | R |
| *D. pettersoni* | 26X-CC | 242.8 | A | G | | | | | F | | | A | R | | | | T | | | C | R | C | C | R | R | | | F | F | | | | | | | | |
| | 27X-CC | 252.4 | A | G | | T | | | R | R | T | A | | | | | | | | | R | C | | R | T | F | | F | T | R | | | | | | | |
| | 28X-CC | 262.1 | A | G | | | | T | | R | | A | | | | R | | T | | C | | | R | | | | | | | R | R | R | | | | | |
| | 29X-CC | 271.7 | C | G | | | | | F | | | F | | | | R | R | | | R | R | C | | | | | R | | F | F | | | | | | | |
| | 30X-CC | 281.3 | R | G | | | | | | | | | | | A | | | | | | R | | | | | R | T | R | | | | | | | | | |
| | 31X-CC | 290.9 | C | G | R | | T | | | | | C | | | A | T | C | T | R | F | R | | | R | R | | | | | | | | | | | | |
| | 32X-CC | 300.5 | A | G | T | T | T | R | C | F | | F | | A | A | R | R | T | C | F | R | R | R | | | | | | | | | | | | | | |
| *D. alata* | 33X-CC | 310.2 | A | G | C | R | R | T | R | C | R | R | T | | | | | | | | | | | | | | | | | | | | | | | | |

Note: See “Explanatory Notes” chapter for abbreviations.

**Table 6 (continued).**

| Zone | Core, section, interval | Depth (mbsf) | Abundance | Preservation | *Cycladophora bicornis* gr. | *Lipmanella virchowii* | *Stylochlamidium venustum* | *Lamprocyclas margatense* | *Stylacontarium acquilonium* | *Eucyrtidium infundibulum* | *Botryostrobus praetumidulus* | *Actinomma popofski* | *Gondwanaria dogeli* | *Pterocanium korotnevi* | *Siphocampe arachnea* | *Eucyrtidium calvertense* | *Pterocanium auritum* | *Eucyrtidium inflatum* | *Lamprocyrtis heteroporos* | *Spongotrochus glacialis* | *Lychnocanoma n. sakai* | *Dictyophimus bullatus* | *Phormostichoartus crustula* | *Dictyophimus crisiae* | *Eucyrtidium erythromystax* | *Sphaeropyle langii* | *Botryostrobus tumidulus* | *Cycladophora davisiana davisiana* | *Sphaeropyle robusta* | *Pseudocubus warreni* | *Lamprocyrtis daniellae* | *Botryostrobus aquilonaris* | *Lamprocyrtis neoheteroporos* | *Eucyrtidium matuyamai* |
|---|---|---|---|---|---|---|---|---|---|---|---|---|---|---|---|---|---|---|---|---|---|---|---|---|---|---|---|---|---|---|---|---|---|---|
| Unzoned | 167-1021B- | | | | | | | | | | | | | | | | | | | | | | | | | | | | | | | | | |
| | 1H-CC | 8.0 | B | | | | | | | | | | | | | | | | | | | | | | | | | | | | | | | |
| | 2H-CC | 17.5 | B | | | | | | | | | | | | | | | | | | | | | | | | | | | | | | | |
| | 3H-CC | 27.0 | R | P | | | | | R | | | | | | | | | | | | | | | | | | | | | | | | | |
| | 4H-CC | 36.5 | B | | | | | | | | | | | | | | | | | | | | | | | | | | | | | | | |
| *E. matuyamai* | 5H-CC | 46.0 | R | P | | | | | R | | R | | | | | | | | | | | | | | | | | | | | | | | R |
| *S. langii* | 6H-CC | 55.5 | A | G | C | T | C | | F | T | | R | | R | | R | F | | F | T | R | | | | | | R | A | R | F | | R | A | |
| | 7H-CC | 65.0 | A | M | C | | F | | R | | | R | | R | | R | | | A | | | | | | T | | | C | R | | | R | R | |
| | 8H-CC | 65.0 | C | M | A | T | R | | R | R | | | T | | | | | | A | | | | | | | T | T | R | R | F | R | | | |
| | 9H-CC | 84.0 | F | G | C | | R | | F | | T | | | | | T | | | A | | | | | | | | | | | | | | | |
| | 10H-CC | 93.5 | R | G | | | | | P | | | | | | | | | | P | | | | | | | | | | | | | | | |
| | 11H-CC | 103.0 | R | G | P | | | | P | | | | | | | | | | P | | P | | | P | | | | | | | | | | |
| | 12H-CC | 112.5 | R | G | P | | | | P | | | | | | | | | | P | | P | | | P | P | P | | | | | | | | |
| *S. peregrina* | 13H-CC | 122.0 | R | G | P | | P | | | | P | | | | | P | | | | | | P | P | | | | | | | | | | | |
| | 14H-CC | 131.0 | R | M | | | | | P | | | | | P | | | | | P | | P | | | | | | | | | | | | | |
| | 15H-CC | 141.0 | A | G | F | | | | | | R | | | R | | R | R | | A | | P | | | | | | | | | | | | | |
| | 16H-CC | 150.5 | C | G | R | | R | | C | | | | | | | | | | A | | T | | | | | | | | | | | | | |
| | 17H-CC | 160.0 | C | G | C | T | | | A | T | F | | | T | | R | | | A | R | | | | | | | | | | | | | | |
| | 18H-CC | 169.5 | A | G | A | | | | | | R | | | R | | R | R | T | | | | | | | | | | | | | | | | |
| | 19X-CC | 175.4 | F | G | C | | | | | | C | T | | | | R | | | | | | | | | | | | | | | | | | |
| | 20X-CC | 185.0 | C | G | C | | | | | | C | R | T | T | R | | | | | | | | | | | | | | | | | | | |
| | 21X-CC | 194.7 | R | M | | | | | | | T | | | | | | | | | | | | | | | | | | | | | | | |
| | 22X-CC | 204.3 | F | G | C | | | | R | R | | | | | | | | | | | | | | | | | | | | | | | | |
| | 23X-CC | 214.0 | A | G | | | | R | R | | | | | | | | | | | | | | | | | | | | | | | | | |
| *D. penultima* | 24X-CC | 223.6 | C | G | F | T | R | T | | | | | | | | | | | | | | | | | | | | | | | | | | |
| | 25X-CC | 233.2 | A | G | | | | | | | | | | | | | | | | | | | | | | | | | | | | | | |
| *D. petterssoni* | 26X-CC | 242.8 | A | G | | | | | | | | | | | | | | | | | | | | | | | | | | | | | | |
| | 27X-CC | 252.4 | A | G | | | | | | | | | | | | | | | | | | | | | | | | | | | | | | |
| | 28X-CC | 262.1 | A | G | | | | | | | | | | | | | | | | | | | | | | | | | | | | | | |
| | 29X-CC | 271.7 | C | G | | | | | | | | | | | | | | | | | | | | | | | | | | | | | | |
| | 30X-CC | 281.3 | R | G | | | | | | | | | | | | | | | | | | | | | | | | | | | | | | |
| | 31X-CC | 290.9 | C | G | | | | | | | | | | | | | | | | | | | | | | | | | | | | | | |
| | 32X-CC | 300.5 | A | G | | | | | | | | | | | | | | | | | | | | | | | | | | | | | | |
| *D. alata* | 33X-CC | 310.2 | A | G | | | | | | | | | | | | | | | | | | | | | | | | | | | | | | |

**Table 7. Radiolarian events at Holes 1021B and 1021C.**

| Label | Event | Hole 1021B Top (mbsf) | Hole 1021B Base (mbsf) | Hole 1021C Top (mbsf) | Hole 1021C Base (mbsf) |
|---|---|---|---|---|---|
| R1 | FO *E. matuyamai* | 46.0 | 55.5 | ? | ? |
| R2 | FO *L. neoheteroporos* | 65.0 | 74.5 | 62.5 | 72.0 |
| R3 | FO *C. d. davisiana* | 74.5 | 84.0 | 72.0 | 81.5 |
| R4 | LO *D. splendens* | 160 | 169.5 | | |
| R5 | FO *L. heteroporos* | 160 | 169.5 | | |
| R6 | FO *S. acquilonium* | 214 | 223.6 | | |
| R7 | LO *L. n. magnacornuta* | 233.2 | 242.8 | | |
| R8 | LO *C. japonica* | 271.7 | 281.3 | | |
| R9 | LO *C. cornuta* | 290.9 | 300.5 | | |

Note: FO = first occurrence, LO = last occurrence.

depth offsets in the composite section. On the composite depth scale (expressed as mcd, meters composite depth), features of the plotted MST and color reflectance data present in adjacent holes are aligned so that they occur at approximately the same depth. Working from the top of the sedimentary sequence, a constant was added to the mbsf (meters below sea floor) depth for each core in each hole to arrive at a mcd depth for that core. The depths offsets that compose the composite depth section are given in Table 10, also on CD-ROM, back pocket. The continuity of the sedimentary sequence was documented for the upper 185 mcd, equivalent to the entire interval that was multiple cored.

Color reflectance, magnetic susceptibility, and GRAPE density measurement were the primary parameters used for interhole correlation purposes. Natural gamma-ray activity measurements were made throughout the entire section in Holes 1021A, 1021B, and 1021C, but the sampling interval of 12 cm was insufficient for interhole correlation.

The color reflectance, magnetic susceptibility, and GRAPE records used to verify core overlap for Site 1021 are shown on a composite depth scale in Figures 10, 11, and 12, respectively. The GRAPE data were used to identify intervals of voids and highly disturbed sediments (values less than 1.50 g/cm$^3$), and all MST and color reflectance data were culled from these intervals. The cores from Holes 1021A through 1021D provide continuous overlap to about 185 mcd. The composite records suggest that up to 2.5 m of material may be missing between cores down to about 185 mcd, although the average gap is about 1 m. As there are no data to fill possible core gaps below 185 mcd, an assessment of core gap length below this depth is not possible.

Following construction of the composite depth section for Site 1021, a single spliced record was assembled from the aligned cores mainly using magnetic susceptibility and GRAPE data, and in some cases, color reflectance data. Cores from Hole 1021B were used as the backbone of the sampling splice. Except for Cores 167-1021D-10H and 11H, cores from Holes 1021C were used to splice across core gaps in Hole 1021B. The composite depths were aligned so that tie points between adjacent holes occurred at exactly the same depths in meters composite depth. The Site 1021 splice (Table 11, also on CD-ROM, back pocket) can be used as a sampling guide to recover a single sedimentary sequence that is continuous down to 185 mcd. Intervals having significant disturbance or distortion were avoided if possible. Core 167-1021B-10H had flow-in structures in Sections 3 through 5. Unfortunately, cores from Holes 1021C and 1021D did not fully span across this interval and a small section (76 cm; see Table 11) of Core 167-1021B-10H had to be used in the splice.

A preliminary age model (Table 12) was constructed to estimate sedimentation rates (Fig. 13). The age model was applied to the spliced records of GRAPE, magnetic susceptibility, and color reflectance shown in Figure 14.

## INORGANIC GEOCHEMISTRY

We collected 15 interstitial water samples from Hole 1021B at depths ranging from 2.96 to 304.95 mbsf, with samples covering the two lithostratigraphic units defined at this site (see "Lithostratigraphy" section, this chapter). Chemical gradients in the interstitial waters at this site (Table 13) reflect organic matter diagenesis, the dissolution of biogenic opal, and possibly the diffusive influence of reactions in the underlying basalt.

Chlorinity increases by 1.8% from 554 mM at 2.96 mbsf to 564 mM at 40.95 mbsf, then decreases with increasing depth to 550–555 mM from 107.45 to 304.95 mbsf (Fig. 15). Salinity, measured refractively as total dissolved solids, ranges from 34.5–35.0. Sodium concentrations measured by flame emission spectrophotometry were on average <0.5% higher than those estimated by charge balance (Table 13).

Alkalinity increases to ≥9 mM from 135.95 to 164.95 mbsf, then decreases with depth to 6.5 mM at 304.95 mbsf (Fig. 15). Sulfate is not completely reduced at this depth, with sulfate concentrations decreasing by over 25% from 27.0 mM at 2.96 mbsf to an average of 19.7 mM from 107.45 to 304.95 mbsf. Phosphate concentrations are >15 µM from 2.96 to 78.95 mbsf, then decrease with increasing depth to 3–5 µM from 247.25 to 304.95 mbsf. Ammonium concentrations increase with increasing depth to >500 µM from 78.95 to 189.45 mbsf, then decrease to 274 µM at 304.95 mbsf. Manganese concentrations are >100 µM from 2.96 to 21.95 mbsf, then decrease to values of 50–70 µM from 78.95 to 304.95 mbsf, consistent with suboxic diagenesis shallow in the sediments and with the incomplete extent of sulfate reduction.

Dissolved silicate concentrations are 380–550 µM from 2.96 to 40.95 mbsf, then increase with depth to values consistently >1000 µM by 218.45 mbsf (Fig. 15), indicative of the dissolution of biogenic opal. Strontium concentrations are approximately seawater values throughout (Table 13).

Calcium concentrations decrease to a minimum of 8.7 mM at 107.45 mbsf, then increase with increasing depth to 12.5 mM in the deepest sample at 304.95 mbsf (Fig. 15). The average calcium gradient from the depth of the calcium minimum is +1.9 mM/100 m. Magnesium concentrations decrease gradually throughout to 47 mM at 304.95 mbsf, with an average gradient from the depth of the calcium minimum of –0.87 mM/100 m. The decrease in dissolved calcium in this upper sediment indicates that authigenic mineral precipitation may be significant in influencing this profile in this depth range, while both profiles apparently reflect the diffusive influence of reactions in underlying basalt at deeper depths. At depths ≥107.45 mbsf, the calcium increase is linearly correlated to the magnesium decrease, with $\Delta Ca/\Delta Mg$ of –2.1 ($R^2 = 0.78$). Potassium concentrations decrease slightly with increasing depth to 9.7–9.8 mM from 164.45 to 304.95 mbsf (Table 13). Lithium concentrations are at or below typical seawater values from 2.96 to 40.95 mbsf, then increase with increasing depth to 50 µM ≥164.45 mbsf (Fig. 15).

## ORGANIC GEOCHEMISTRY

Organic geochemical analyses performed at Site 1021 include measurements of elemental composition and volatile hydrocarbons (for methods see "Organic Geochemistry" section, "Explanatory Notes" chapter, this volume).

### Volatile Hydrocarbons

As part of the shipboard safety and pollution program, volatile hydrocarbons (methane, ethane, and propane) in the sediments at Site 1021 were routinely measured by gas chromatography. Headspace

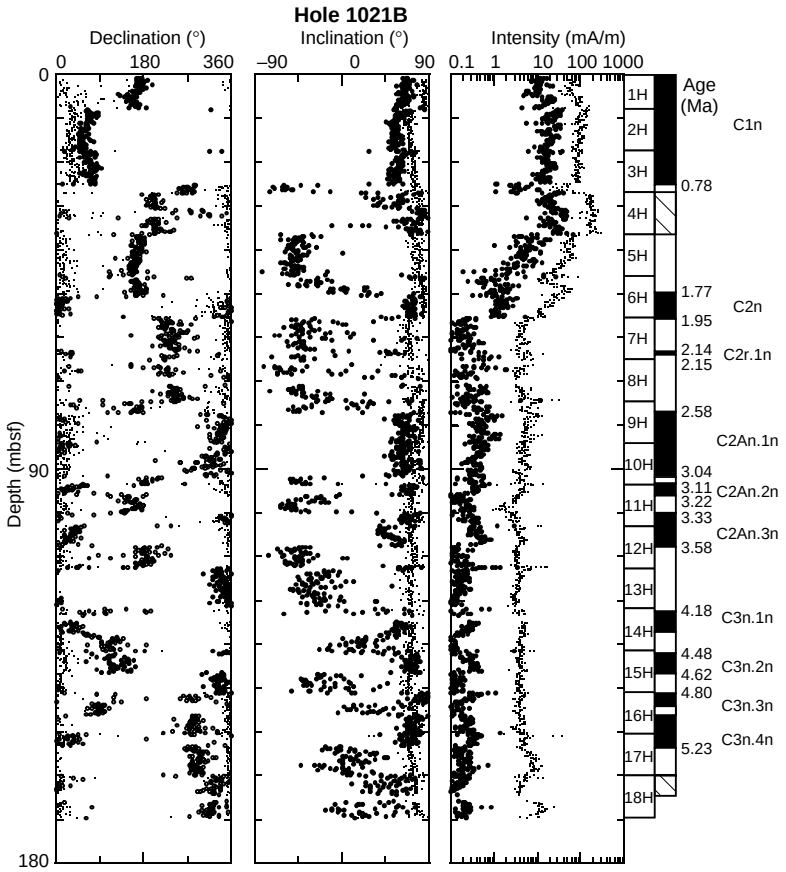


Figure 7. Plots of magnetic declination, inclination, and intensity of APC cores from Hole 1021B. Small and large dots represent the data before and after AF demagnetization at 20 mT, respectively. Open symbols in the declination plot represent values corrected for orientation with the Tensor tool. Identification of polarity chrons and age assignments are shown on the right (Cande and Kent, 1995).

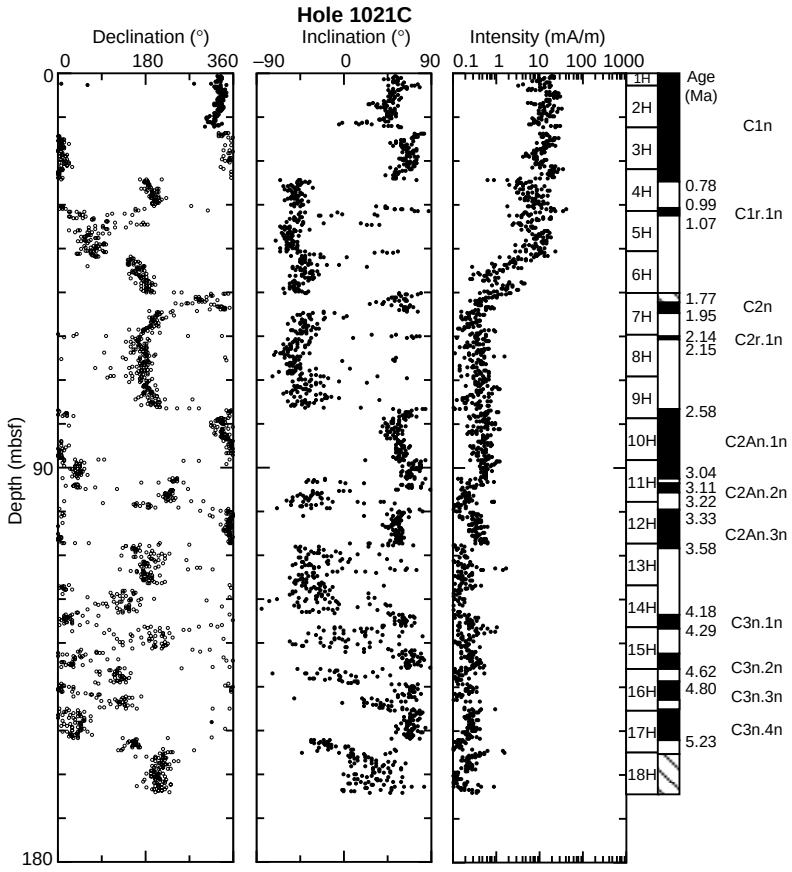


Figure 8. Plots of magnetic declination, inclination, and intensity of APC cores from Hole 1021C obtained after AF demagnetization at 20 mT (solid symbols). Open symbols in the declination plot represent values corrected for orientation by the Tensor tool. Identification of polarity chrons and age assignments are shown on the right (Cande and Kent, 1995).

**Table 8. Magnetostratigraphic datum levels in Hole 1021B.**

| Chronozone boundary | Age (Ma) | Upper limit | | | Lower limit | | |
|---|---|---|---|---|---|---|---|
| | | Core, section | Level (cm) | Depth (mbsf) | Core, section | Level (cm) | Depth (mbsf) |
| | | 167-1021B- | | | 167-1021B- | | |
| C1n Brunhes (o) | 0.780 | 3H-6 | 15 | 25.15 | 3H-6 | 25 | 25.25 |
| C1r.1n Jaramillo (t) | 0.990 | | | | | | |
| C1r.1n Jaramillo (o) | 1.070 | | | | | | |
| C2n Olduvai (t) | 1.770 | 6H-2 | 105 | 48.55 | 6H-3 | 105 | 50.05 |
| C2n Olduvai (o) | 1.950 | 7H-1 | 35 | 55.85 | 7H-1 | 45 | 55.95 |
| C2r.1n Reunion (t) | 2.140 | 7H-5 | 145 | 62.95 | 7H-6 | 25 | 63.25 |
| C2r.1n Reunion (o) | 2.150 | 7H-6 | 105 | 64.05 | 7H-6 | 125 | 64.25 |
| C2An.1n Gauss (t) | 2.581 | 9H-2 | 105 | 77.05 | 9H-2 | 135 | 77.35 |
| C2An.1r Kaena (t) | 3.040 | 10H-6 | 35 | 91.85 | 10H-6 | 65 | 92.15 |
| C2An.1r Kaena (o) | 3.110 | 10H-7 | 65 | 93.65 | 11H-1 | 15 | 93.65 |
| C2An.2r Mammoth (t) | 3.220 | 11H-2 | 105 | 96.05 | 11H-2 | 125 | 96.25 |
| C2An.2r Mammoth (o) | 3.330 | 11H-5 | 35 | 99.85 | 11H-5 | 65 | 100.15 |
| C2Ar Gilbert (t) | 3.580 | 12H-4 | 25 | 107.75 | 12H-4 | 35 | 107.85 |
| C3n.1n Cochiti (t) | 4.180 | 13H-6 | 125 | 121.25 | 14H-1 | 125 | 123.25 |
| C3n.1n Cochiti (o) | 4.290 | | | | | | |
| C3n.2n Nunivak (t) | 4.480 | 14H-7 | 25 | 131.25 | 15H-1 | 55 | 132.05 |
| C3n.2n Nunivak (o) | 4.620 | 15H-4 | 75 | 136.75 | 15H-4 | 85 | 136.85 |
| C3n.3n Sidufjall (t) | 4.800 | 15H-7 | 55 | 141.05 | 16H-1 | 5 | 141.05 |
| C3n.3n Sidufjall (o) | 4.890 | | | | | | |
| C3n.4n Thvera (t) | 4.980 | | | | | | |
| C3n.4n Thvera (o) | 5.230 | 17H-2 | 135 | 153.35 | 17H-3 | 15 | 153.65 |
| C3A.n1 (t) | 5.894 | | | | | | |

Notes: o = onset; t = termination; the assigned ages of the reversal boundaries are according to the time scale of Cande and Kent (1995). The upper and lower limits define the range within which a reversal occurs.

**Table 9. Magnetostratigraphic datum levels in Hole 1021C.**

| Chronozone boundary | Age (Ma) | Upper limit | | | Lower limit | | |
|---|---|---|---|---|---|---|---|
| | | Core, section | Level (cm) | Depth (mbsf) | Core, section | Level (cm) | Depth (mbsf) |
| | | 167-1021C- | | | 167-1021C- | | |
| C1n Brunhes (o) | 0.780 | 4H-2 | 115 | 24.25 | 4H-2 | 125 | 24.35 |
| C1r.1n Jaramillo (t) | 0.990 | 4H-6 | 115 | 30.25 | 4H-6 | 135 | 30.45 |
| C1r.1n Jaramillo (o) | 1.070 | 5H-1 | 35 | 31.45 | 5H-2 | 15 | 32.75 |
| C2n Olduvai (t) | 1.770 | 6H-7 | 65 | 50.25 | 7H-2 | 95 | 52.46 |
| C2n Olduvai (o) | 1.950 | 7H-3 | 125 | 54.26 | 7H-3 | 145 | 54.46 |
| C2r.1n Reunion (t) | 2.140 | 7H-7 | 55 | 59.56 | 8H-1 | 15 | 59.75 |
| C2r.1n Reunion (o) | 2.150 | 8H-1 | 75 | 60.35 | 8H-1 | 95 | 60.55 |
| C2An.1n Gauss (t) | 2.581 | 9H-5 | 105 | 76.15 | 9H-6 | 25 | 76.85 |
| C2An.1r Kaena (t) | 3.040 | 11H-3 | 135 | 92.45 | 11H-4 | 5 | 92.65 |
| C2An.1r Kaena (o) | 3.110 | 11H-4 | 65 | 93.25 | 11H-4 | 125 | 93.85 |
| C2An.2r Mammoth (t) | 3.220 | 11H-5 | 75 | 94.85 | 11H-5 | 135 | 95.45 |
| C2An.2r Mammoth (o) | 3.330 | 12H-2 | 5 | 99.15 | 12H-2 | 45 | 99.55 |
| C2Ar Gilbert (t) | 3.580 | 12H-7 | 75 | 107.35 | 13H-1 | 95 | 108.05 |
| C3n.1n Cochiti (t) | 4.180 | 14H-5 | 35 | 122.95 | 14H-5 | 65 | 123.25 |
| C3n.1n Cochiti (o) | 4.290 | 14H-7 | 65 | 126.25 | 15H-1 | 25 | 126.35 |
| C3n.2n Nunivak (t) | 4.480 | | | | | | |
| C3n.2n Nunivak (o) | 4.620 | 16H-1 | 5 | 135.65 | 16H-1 | 25 | 135.85 |
| C3n.3n Sidufjall (t) | 4.800 | 16H-2 | 115 | 138.25 | 16H-3 | 65 | 139.25 |
| C3n.3n Sidufjall (o) | 4.890 | | | | | | |
| C3n.4n Thvera (t) | 4.980 | | | | | | |
| C3n.4n Thvera (o) | 5.230 | 17H-5 | 75 | 151.85 | 17H-5 | 95 | 152.05 |
| C3A.n1 (t) | 5.894 | | | | | | |

Notes: o = onset; t = termination; the assigned ages of the reversal boundaries are according to the time scale of Cande and Kent (1995). The upper and lower limits define the range within which a reversal occurs.

methane concentrations were near the laboratory air concentration (less than 5 ppm) throughout the entire hole. This indicates that no methanogenesis has occurred at this site.

## Elemental Analysis

At Site 1021, 107 sediment samples were analyzed for total carbon, inorganic carbon, total nitrogen, and total sulfur (Table 14, also on CD-ROM, back pocket; Fig. 16).

The percentage of calcium carbonate ($CaCO_3$) was calculated from inorganic carbon concentrations by assuming that all carbonate occurs in the form of calcite. Generally, the calcium carbonate contents vary between ~0 and 60 wt%. Two intervals (86–105 mbsf and 222–275 mbsf) show distinctly elevated $CaCO_3$ contents up to ~60 wt%, which correlate with zones of well-preserved calcareous microfossils (see "Biostratigraphy" section, this chapter). In contrast, the low $CaCO_3$ content of two intervals (0–86 mbsf and 105–275 mbsf) is attributed to the dissolution of carbonates, which is suggested by the poor preservation of calcareous organisms (see "Biostratigraphy" section, this chapter).

The total organic carbon (TOC) content at Site 1021 varies between 0 and 0.6 wt% (Table 14; Fig. 16) and decreases downhole. Both the low TOC content and the downhole decrease of TOC are commonly observed in open marine deep-sea sediments. The decrease of TOC is likely caused by the degradation of labile organic matter during diagenesis.

Total nitrogen content varies between 0.06 and 0.17 wt%, and total sulfur content ranges from 0 to ~0.3 wt% (Table 14). Most of the total organic carbon/total nitrogen (TOC/TN) ratios range between 1 and 5 and decrease downhole. This pattern seems to reflect the decrease of TOC concentration. The low TOC/TN ratios indicate a predominant marine origin of the organic material (Bordovskiy, 1965;

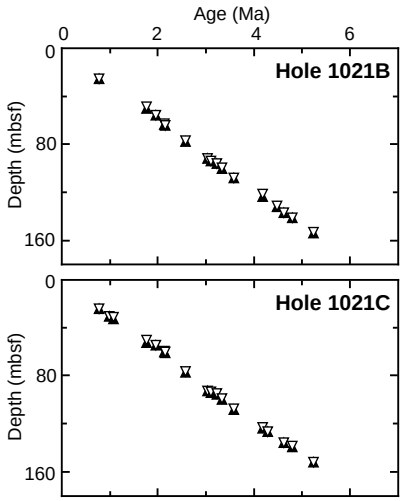


Figure 9. Age/depth plots based on geomagnetic reversal boundaries of Holes 1021B and 1021C. The sedimentation rate is exceptionally constant at 30 m/m.y. over more than 5 m.y. Open and solid triangles show the upper and lower limits of the magnetostratigraphic reversal boundaries.

Emerson and Hedges, 1988). In organic carbon–lean sediments, however, TOC/TN ratios have to be interpreted very carefully, because inorganic nitrogen in ammonium ions can be absorbed by clay minerals and may contribute to the total nitrogen content (Müller, 1977). Thus, the composition of the organic material must be further investigated with shore-based organic geochemical analyses.

## PHYSICAL PROPERTIES

### Multisensor Track Measurements

The shipboard physical properties program at Site 1021 included nondestructive measurements of bulk density, magnetic susceptibility, *P*-wave velocity, and natural gamma-ray activity on whole sections of all cores using the MST (Fig. 17). Magnetic susceptibility was measured at 4-cm intervals at low sensitivity (1-s measuring time) on all Site 1021 cores. GRAPE bulk density measurements were made at 4-cm intervals on all cores from Site 1021. PWL velocity measurements were made at 4-cm intervals on cores from Holes 1021A, 1021C, and 1021D and through Core 167-1021B-19X. Natural gamma-ray activity was measured with a 15-s count every 12 cm on all cores from Site 1021.

### Index Properties

Index properties measurements were made at one sample per working section on all cores from Hole 1021B. The index properties bulk density, void ratio, porosity, water content, dry-bulk density, and grain density were determined using gravimetric Method C (Table 15 on CD-ROM in the back pocket of this volume). Generally, index properties trends (Fig. 18) correspond very well to the variations in lithology (see “Lithostratigraphy” section, this chapter). Grain density in the nannofossil-rich interval (0–110 mbsf) was relatively constant, whereas lower grain densities and slightly higher porosities, both with increased scatter, were measured in the siliceous fossil-rich unit (110–310 mbsf), where diatoms form the main biogenic component (Fig. 18). Throughout the entire section, there are also distinctive oscillations in index properties resulting from varying amounts of clay.

**Table 10. Site 1021 composite depth section.**

| Core, section | Depth (mbsf) | Offset (m) | Depth (mcd) |
|---|---|---|---|
| 167-1021A- | | | |
| 1H-1 | 0.00 | 3.04 | 3.04 |
| 167-1021B- | | | |
| 1H-1 | 0.00 | 0.00 | 0.00 |
| 2H-1 | 8.00 | 1.18 | 9.18 |
| 3H-1 | 17.50 | 1.94 | 19.44 |
| 4H-1 | 27.00 | 2.50 | 29.50 |
| 5H-1 | 36.50 | 4.02 | 40.52 |
| 6H-1 | 46.00 | 4.76 | 50.76 |
| 7H-1 | 55.50 | 5.69 | 61.19 |
| 8H-1 | 65.00 | 6.55 | 71.55 |
| 9H-1 | 74.50 | 8.71 | 83.21 |
| 10H-1 | 84.00 | 12.75 | 96.75 |
| 11H-1 | 93.50 | 13.15 | 106.65 |
| 12H-1 | 103.00 | 14.31 | 117.31 |
| 13H-1 | 112.50 | 14.29 | 126.79 |
| 14H-1 | 122.00 | 13.43 | 135.43 |
| 15H-1 | 131.50 | 14.13 | 145.63 |
| 16H-1 | 141.00 | 14.95 | 155.95 |
| 17H-1 | 150.50 | 15.53 | 166.03 |
| 18H-1 | 160.00 | 15.41 | 175.41 |
| 19X-1 | 169.50 | 15.41 | 184.91 |
| 20X-1 | 175.40 | 15.41 | 190.81 |
| 21X-1 | 185.00 | 15.41 | 200.41 |
| 22X-1 | 194.70 | 15.41 | 210.11 |
| 23X-1 | 204.30 | 15.41 | 219.71 |
| 24X-1 | 214.00 | 15.41 | 229.41 |
| 25X-1 | 223.60 | 15.41 | 239.01 |
| 26X-1 | 233.20 | 15.41 | 248.61 |
| 27X-1 | 242.80 | 15.41 | 258.21 |
| 28X-1 | 252.40 | 15.41 | 267.81 |
| 29X-1 | 262.20 | 15.41 | 277.61 |
| 30X-1 | 271.70 | 15.41 | 287.11 |
| 31X-1 | 281.30 | 15.41 | 296.71 |
| 32X-1 | 290.90 | 15.41 | 306.31 |
| 33X-1 | 300.50 | 15.41 | 315.91 |
| 167-1021C- | | | |
| 1H-1 | 0.00 | –0.08 | –0.08 |
| 2H-1 | 2.60 | 0.88 | 3.48 |
| 3H-1 | 12.10 | 0.44 | 12.54 |
| 4H-1 | 21.60 | 2.88 | 24.48 |
| 5H-1 | 31.10 | 4.12 | 35.22 |
| 6H-1 | 40.60 | 5.24 | 45.84 |
| 7H-1 | 50.10 | 6.64 | 56.74 |
| 8H-1 | 59.60 | 9.19 | 68.79 |
| 9H-1 | 69.10 | 9.64 | 78.74 |
| 10H-1 | 78.60 | 10.84 | 89.44 |
| 11H-1 | 88.10 | 13.96 | 102.06 |
| 12H-1 | 97.60 | 13.78 | 111.38 |
| 13H-1 | 107.10 | 13.75 | 120.85 |
| 14H-1 | 116.60 | 14.21 | 130.81 |
| 15H-1 | 126.10 | 15.09 | 141.19 |
| 16H-1 | 135.60 | 16.59 | 152.19 |
| 17H-1 | 145.10 | 16.99 | 162.09 |
| 18H-1 | 154.60 | 19.65 | 174.25 |
| 167-1021D- | | | |
| 1H-1 | 0.00 | –0.04 | –0.04 |
| 2H-1 | 5.50 | 1.40 | 6.90 |
| 3H-1 | 15.00 | 2.82 | 17.82 |
| 4H-1 | 24.50 | 3.02 | 27.52 |
| 5H-1 | 34.00 | 3.82 | 37.82 |
| 6H-1 | 43.50 | 4.90 | 48.40 |
| 7H-1 | 53.00 | 6.65 | 59.65 |
| 8H-1 | 62.50 | 6.85 | 69.35 |
| 9H-1 | 72.00 | 8.52 | 80.52 |
| 10H-1 | 81.50 | 9.06 | 90.56 |
| 11H-1 | 91.00 | 9.37 | 100.37 |
| 12H-1 | 100.50 | 10.74 | 111.24 |
| 13H-1 | 110.00 | 14.61 | 124.61 |
| 14H-1 | 119.50 | 15.07 | 134.57 |
| 15H-1 | 129.00 | 16.05 | 145.05 |

Note: This table is also on CD-ROM, back pocket, this volume.

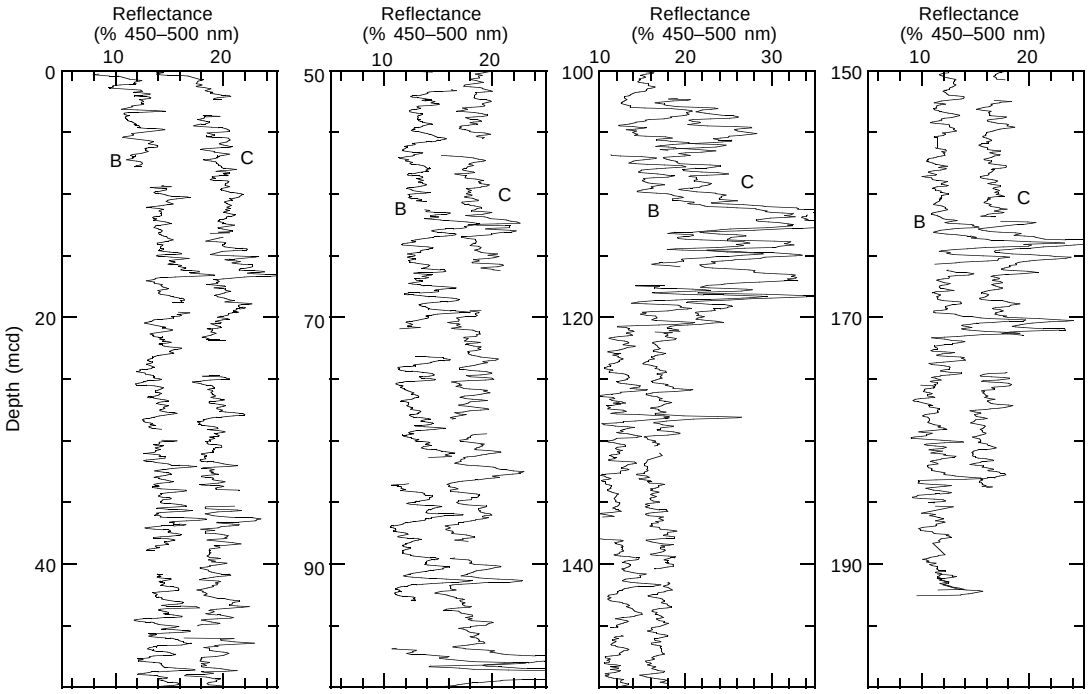


Figure 10. Smoothed (15-cm Gaussian) color reflectance (% 450–500 nm band) data for the upper 200 m from Site 1021 on the mcd scale. Holes 1021B and Hole 1021C are offset from each other by a constant (5%). Note different vertical scale used for the 100–150 mcd panel.

## Compressional-Wave Velocity

*P*-wave velocity was measured with the Hamilton Frame (pair T3, in the x-direction), generally twice per core, to 301.05 mbsf in Hole 1021B (Table 16 on CD-ROM in the back pocket of this volume). Values range from 1472 to 1653 m/s, showing a gradual increase with depth (Fig. 19).

## Heat Flow

Thermal conductivity was measured to 86.85 mbsf in Hole 1021C (Table 17 on CD-ROM in the back pocket of this volume). Three downhole temperature measurements were taken with the APC Adara temperature tool in Hole 1021B: 3.7°C at 36.5 mbsf, 4.1°C at 52.5 mbsf, and 5.7°C at 84.0 mbsf in Cores 167-1021B-4H, 6H, and 9H, respectively (Fig. 20). Bottom-water temperature was measured on all runs, indicating a bottom-water temperature of 1.1°C ± 0.1°C. The four data points yield a thermal gradient of 54°C/km (Fig. 21). Using an average measured thermal conductivity of 0.849 W/(m·K) provides a heat-flow estimate of 46 mW/m$^2$ at Site 1021.

## Color Reflectance

Reflectance measurements were taken at 4- to 6-cm intervals on cores from Holes 1021B and 1021C. The color reflectance data are consistent with the major lithostratigraphic units at this site. A summary for the blue band (450–500 nm) and the near infrared (850–900 nm) to blue ratio is given in Figure 22. In the portion of lithostratigraphic Unit I dominated by clay, the reflectance signal is flat for the 450–500-nm band (average 14%) and the ratio of near infrared over blue ranges from 0.8 to 1.1. From 80 to 110 mbsf in lithostratigraphic Unit I, where nannofossils are relatively abundant, color reflectance is slightly higher (average 20%). Lithostratigraphic Subunit IIB, which is dominated by diatomaceous sediments, shows high but variable reflectance for the 450–500-nm band (10%–35%) and the near infrared/blue ratio (0.6–1.4). Peaks in nannofossil content correspond to maxima in blue reflectance at 237 and 305 mbsf.

## Digital Color Video

Cores from all holes at Site 1021 were imaged with the ODP color digital imaging system at 20-cm intervals downcore, providing a 0.25-mm pixel. Video images of color CIELAB L* from Holes 1021A, 1021B, 1021C, and 1021D are shown in Figure 23.

## SUMMARY

Site 1021 in the Delgada Fan region, which provided a longer, lower-resolution sedimentary section in the Gorda Transect, was drilled on a small rise that appeared to be hemipelagic based upon seismic reflection profiles (Fig. 24). It was drilled on oceanic crust of late Oligocene age, with the objective to drill as much of the Neogene section as time permitted. Despite drilling 310 m out of a total estimated 385-m sediment column, the oldest recovered sediments were late middle Miocene in age (~11.8 Ma). Given the basement age, significantly slower sedimentation and/or gaps in deposition must have occurred below the section drilled. Site 1021 was triple cored to a depth of 139 mbsf (~4.8 Ma) and double cored to 164 mbsf (~5.8 Ma). A continuous sediment section was established to the base of the double-cored section. Excellent magnetostratigraphy to a depth of 155 mbsf and good biostratigraphy from all microfossil groups for the entire sediment column provided shipboard age control. The sedimentation rate from the late/middle Miocene boundary to the present was essentially constant, at 29 m/m.y. The sedimentation rate in the lowermost sediments recovered was somewhat slower, however. Siliceous biogenic sediments dominate the middle and upper Miocene sediment column, but the sediments abruptly become dominated by

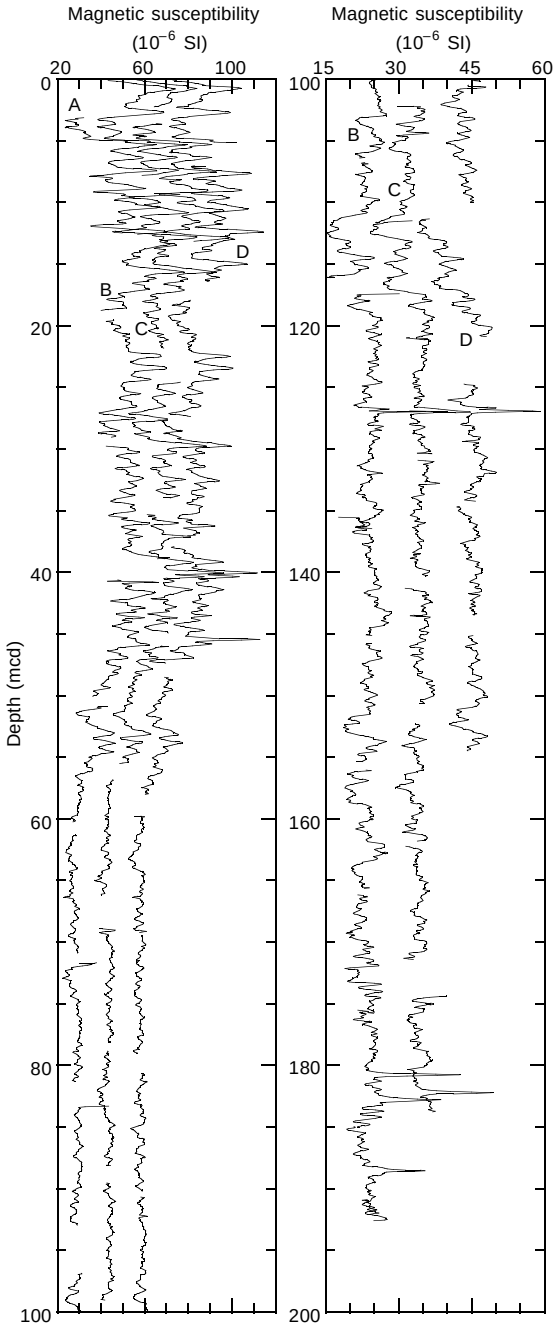


Figure 11. Smoothed (15-cm Gaussian) magnetic susceptibility data for the upper 200 m from Site 1021 on the mcd scale. Holes 1021A, 1021B, 1021C, and 1021D are offset from each other by a constant ($15 \times 10^{-6}$ SI on the 0–100 mcd panel and $10 \times 10^{-6}$ SI on the 100–200 mcd panel). Note different vertical scale used on the two panels.

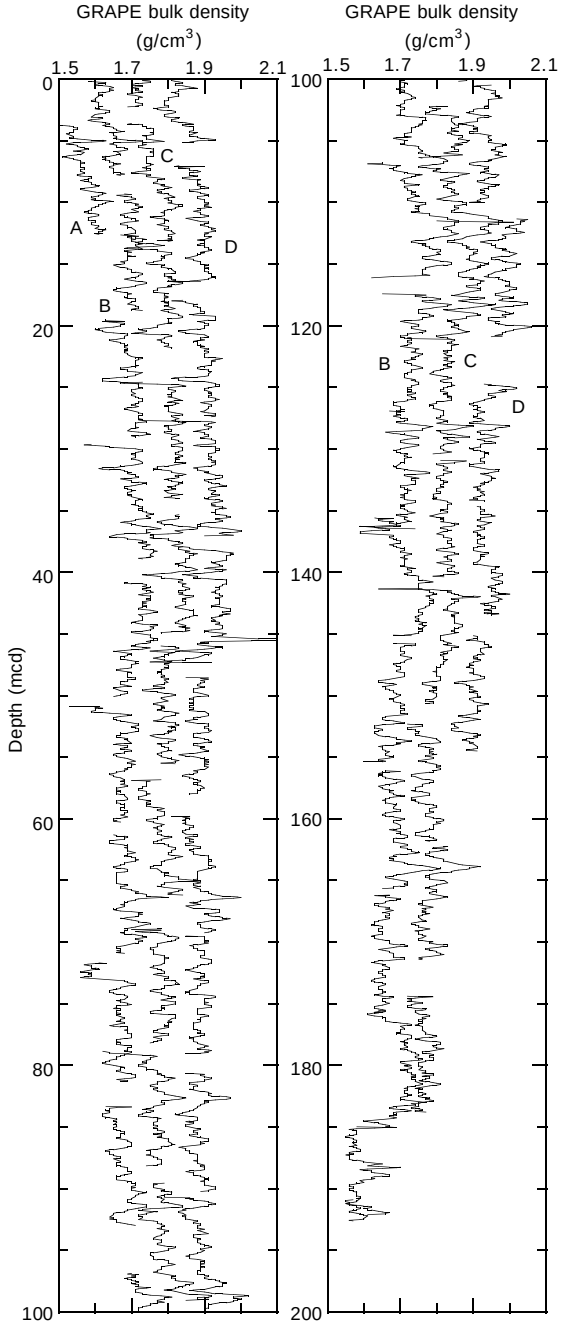


Figure 12. Smoothed (15-cm Gaussian) GRAPE bulk density data for the upper 200 m from Site 1021 on the mcd scale. Holes 1021A, 1021B, 1021C, and 1021D are offset from each other by a constant (0.1 g/cm$^3$).

aluminosilicates at ~ 7 Ma. This is about the same time that Site 1011 experienced this transition, but is roughly two million years older than the transition at Sites 1010 and 1016. The upper Pliocene interval is relatively calcium carbonate-rich, as in other Leg 167 sites, and the calcium carbonate content is significantly lower in the upper Pleistocene sediments.

## REFERENCES

Atwater, T., and Severinghaus, J., 1989. Tectonic map of the northeast Pacific Ocean. *In* Winterer, E.L., Hussong, D.M., and Decker, R.W. (Eds.) *The Eastern Pacific Ocean and Hawaii.* Geol. Soc. Am., Decade of North Am. Geol., Vol. N.

Bordovskiy, O.K., 1965. Accumulation and transformation of organic substances in marine sediment, 2. Sources of organic matter in marine basins. *Mar. Geol.*, 3:5–31.

Cande, S.C., and Kent, D.V., 1995. Revised calibration of the geomagnetic polarity timescale for the Late Cretaceous and Cenozoic. *J. Geophys. Res.*, 100:6093–6095.

Emerson, S., and Hedges, J.I., 1988. Processes controlling the organic carbon content of open ocean sediments. *Paleoceanography*, 3:621–634.

Ingle, J.C., Jr., 1973. Summary comments on Neogene biostratigraphy, physical stratigraphy, and paleo-oceanography in the marginal northeastern Pacific Ocean. *In* Kulm, L.D., von Huene, R., et al., *Init. Repts. DSDP*, 18: Washington (U.S. Govt. Printing Office), 949–960.

Lyle, M., Gallaway, P.J., Liberty, L.M., Mix, A., Stott, L., Hammond, D., Gardner, J., Dean, W., and the EW9504 Scientific Party, 1995a. Data submission. W9406 and EW9504 site surveys of the California margin proposed drillsites, Leg 167 (Vol. 1): Site maps and descriptions. Boise State Univ., *CGISS Tech. Rep.*, 95–11.

————, 1995b. Data submission. W9406 and EW9504 site surveys of the California margin proposed drillsites, Leg 167 (Vol. 2): Seismic profiles. Boise State Univ., *CGISS Tech. Rep.*, 95–12.

McManus, D.A., Burns, R.E., et al., 1970. *Init. Repts. DSDP*, 5: Washington (U.S. Govt. Printing Office).

Müller, P.J., 1977. C/N ratios in Pacific deep sea sediments: effect of inorganic ammonium and organic nitrogen compounds sorbed by clays. *Geochim. Cosmochim. Acta*, 41:765–776.

Rea, D.K., Ness, G.E., and Heath, G.R., 1985. Hemipelagic sedimentation in a region of crustal doming between the Mendocino and Pioneer Fracture Zones. *Mar. Geol.*, 62:69–84.

**Ms 167IR-115**

**NOTE: For all sites drilled, core-description forms ("barrel sheets") and core photographs can be found in Section 3, beginning on page 499. Smear-slide data can be found in Section 4, beginning on page 1327. See Table of Contents for material contained on CD-ROM.**

**Table 11. Site 1021 splice tie points.**

| Hole, core, section, interval (cm) | Depth (mbsf) | Depth (mcd) | | Hole, core, section, interval (cm) | Depth (mbsf) | Depth (mcd) |
|---|---|---|---|---|---|---|
| 1021B-1H-5, 59 | 6.59 | 6.59 | tie to | 1021C-2H-3, 11 | 5.71 | 6.59 |
| 1021C-2H-6, 139 | 11.49 | 12.37 | tie to | 1021B-2H-3, 19 | 11.19 | 12.37 |
| 1021B-2H-5, 135 | 15.35 | 16.53 | tie to | 1021C-3H-3, 99 | 16.09 | 16.53 |
| 1021C-3H-6, 31 | 19.91 | 20.35 | tie to | 1021B-3H-1, 91 | 18.41 | 20.35 |
| 1021B-3H-5, 7 | 23.57 | 25.51 | tie to | 1021C-4H-1, 103 | 22.63 | 25.51 |
| 1021C-4H-4, 127 | 27.37 | 30.25 | tie to | 1021B-4H-1, 75 | 27.75 | 30.25 |
| 1021B-4H-6, 7 | 34.57 | 37.07 | tie to | 1021C-5H-2, 35 | 32.95 | 37.07 |
| 1021C-5H-6, 95 | 39.55 | 43.67 | tie to | 1021B-5H-3, 15 | 39.65 | 43.67 |
| 1021B-5H-5, 71 | 43.21 | 47.23 | tie to | 1021C-6H-1, 139 | 41.99 | 47.23 |
| 1021C-6H-7, 7 | 49.67 | 54.91 | tie to | 1021B-6H-3, 115 | 50.15 | 54.91 |
| 1021B-6H-6, 39 | 53.89 | 58.65 | tie to | 1021C-7H-2, 23 | 51.74 | 58.65 |
| 1021C-7H-4, 119 | 55.70 | 62.61 | tie to | 1021B-7H-2, 7 | 57.07 | 62.76 |
| 1021B-7H-6, 91 | 63.91 | 69.60 | tie to | 1021C-8H-1, 83 | 60.43 | 69.62 |
| 1021C-8H-7, 19 | 68.79 | 77.98 | tie to | 1021B-8H-5, 43 | 71.43 | 77.98 |
| 1021B-8H-7, 39 | 74.39 | 80.94 | tie to | 1021C-9H-2, 71 | 71.31 | 80.95 |
| 1021C-9H-4, 75 | 74.35 | 83.99 | tie to | 1021B-9H-1, 79 | 75.29 | 84.00 |
| 1021B-9H-6, 67 | 82.67 | 91.38 | tie to | 1021C-10H-2, 47 | 80.57 | 91.41 |
| 1021C-10H-6, 131 | 87.41 | 98.25 | tie to | 1021D-10H-6, 19 | 89.19 | 98.25 |
| 1021D-10H-7, 39 | 90.89 | 99.95 | tie to | 1021B-10H-3, 23 | 87.23 | 99.98 |
| 1021B-10H-3, 99 | 87.99 | 100.74 | tie to | 1021D-11H-1, 39 | 91.39 | 100.76 |
| 1021D-11H-5, 139 | 98.39 | 107.76 | tie to | 1021B-11H-1, 111 | 94.61 | 107.76 |
| 1021B-11H-6, 79 | 101.79 | 114.94 | tie to | 1021C-12H-3, 59 | 101.19 | 114.97 |
| 1021C-12H-5, 59 | 104.19 | 117.97 | tie to | 1021B-12H-1, 67 | 103.67 | 117.98 |
| 1021B-12H-6, 27 | 110.77 | 125.08 | tie to | 1021C-13H-3, 123 | 111.33 | 125.08 |
| 1021C-13H-5, 103 | 114.13 | 127.88 | tie to | 1021B-13H-1, 111 | 113.61 | 127.90 |
| 1021B-13H-5, 83 | 119.33 | 133.62 | tie to | 1021C-14H-2, 131 | 119.41 | 133.62 |
| 1021C-14H-4, 83 | 121.93 | 136.14 | tie to | 1021B-14H-1, 71 | 122.71 | 136.14 |
| 1021B-14H-6, 39 | 129.89 | 143.32 | tie to | 1021C-15H-2, 63 | 128.23 | 143.32 |
| 1021C-15H-6, 127 | 134.87 | 149.96 | tie to | 1021B-15H-3, 135 | 135.85 | 149.98 |
| 1021B-15H-5, 135 | 138.85 | 152.98 | tie to | 1021C-16H-1, 79 | 136.39 | 152.98 |
| 1021C-16H-3, 139 | 139.99 | 156.58 | tie to | 1021B-16H-1, 63 | 141.63 | 156.58 |
| 1021B-16H-7, 15 | 150.15 | 165.10 | tie to | 1021C-17H-3, 7 | 148.17 | 165.16 |
| 1021C-17H-4, 43 | 150.03 | 167.02 | tie to | 1021B-17H-1, 99 | 151.49 | 167.02 |
| 1021B-17H-6, 139 | 159.39 | 174.92 | tie to | 1021C-18H-1, 67 | 155.27 | 174.92 |
| 1021C-18H-5, 127 | 161.87 | 181.52 | tie to | 1021B-18H-5, 11 | 166.11 | 181.52 |
| 1021B-18H-7, 63 | 169.63 | 185.04 | | | | |

Note: This table is also on CD-ROM, back pocket, this volume.

**Table 12. Site 1021 sedimentation rate age control points.**

| Event | Depth (mcd) | Age (Ma) |
|---|---|---|
| B Brunhes | 27.16 | 0.78 |
| T Jaramillo | 33.23 | 0.99 |
| T Olduvai | 55.33 | 1.77 |
| T Reunion | 67.54 | 2.14 |
| T Gauss | 86.03 | 2.58 |
| B Kaena | 107.16 | 3.11 |
| B Mammoth | 113.14 | 3.33 |
| T Gilbert | 121.80 | 3.58 |
| T Cochiti | 136.50 | 4.18 |
| T Nunivak | 143.15 | 4.48 |
| T Sidufjall | 155.67 | 4.80 |
| B Thvera | 168.99 | 5.23 |
| T *T. schraderi* | 224.56 | 7.40 |
| B *M. convallis* | 272.66 | 9.46 |
| T *C. japonica* | 291.91 | 10.05 |
| T *C. cornuta* | 311.11 | 11.82 |

Note: T = top, B = bottom.

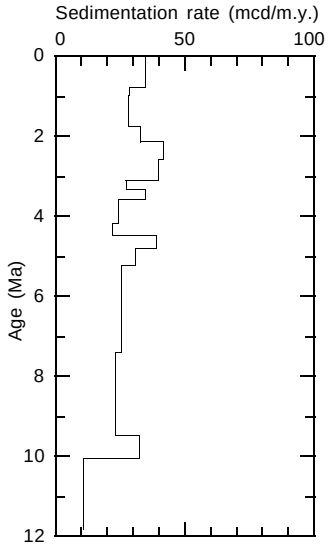


Figure 13. Sedimentation rate vs. age based on the age control points from Table 12.

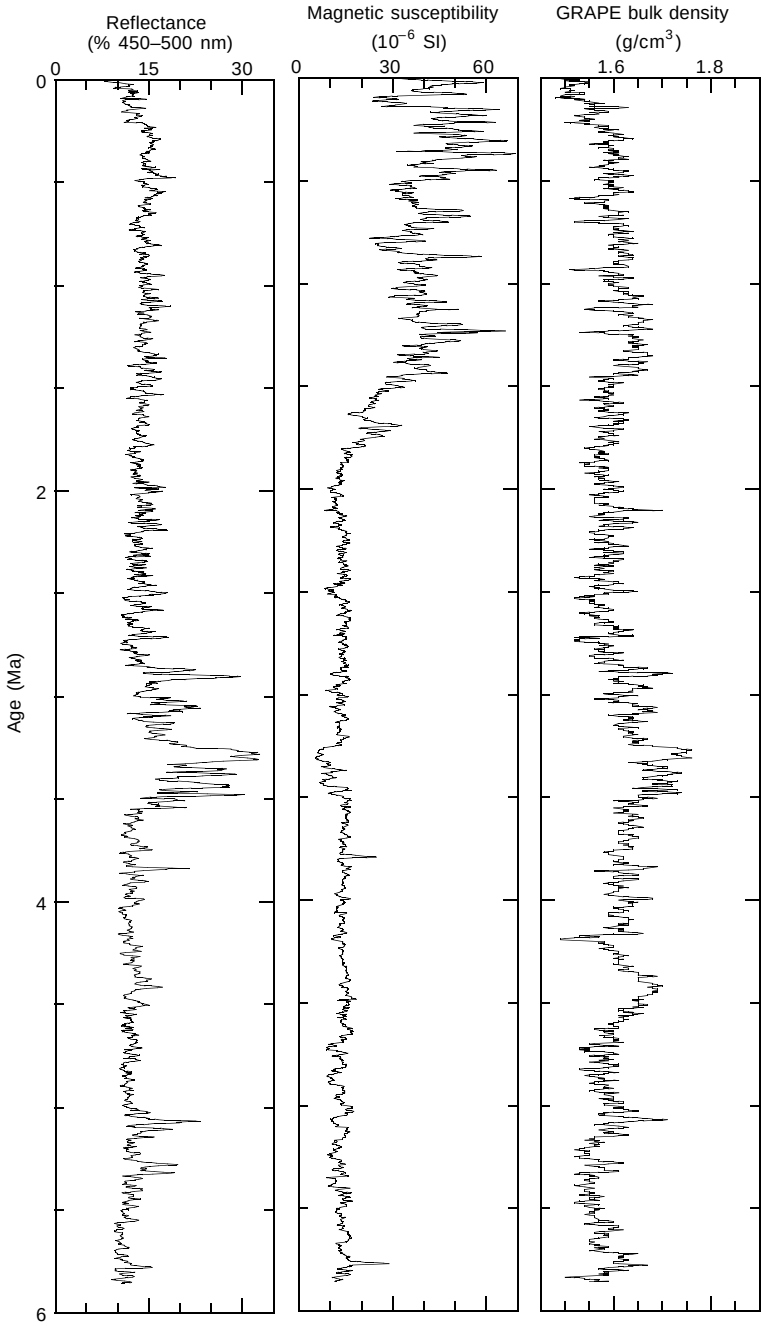


Figure 14. Spliced records of Site 1021 color reflectance, magnetic susceptibility, and GRAPE bulk density vs. age based on age control points from Table 12.

**Table 13. Interstitial water geochemical data, Hole 1021B.**

| Core, section, interval (cm) | Depth (mbsf) | pH | Alkalinity (mM) | Salinity | $Cl^-$ (mM) | $Na^+$ (mM) | $SO_4^{2-}$ (mM) | $HPO_4^{2-}$ (µM) | $NH_4^+$ (µM) | $Mn^{2+}$ (µM) | $H_4SiO_4$ (µM) | $Ca^{2+}$ (mM) | $Mg^{2+}$ (mM) | $Sr^{2+}$ (µM) | $Li^+$ (µM) | $K^+$ (mM) |
|---|---|---|---|---|---|---|---|---|---|---|---|---|---|---|---|---|
| 167-1021B- | | | | | | | | | | | | | | | | |
| 1H-2, 146–150 | 2.96 | 7.55 | 4.07 | 35.0 | 554 | 478 | 27.0 | 21.5 | 64 | 126 | 456 | 10.3 | 51.1 | 82 | 22 | 10.7 |
| 2H-3, 145–150 | 12.45 | 7.34 | 5.65 | 35.0 | 557 | 480 | 25.4 | 19.0 | 214 | 121 | 383 | 10.3 | 50.8 | 82 | 23 | 10.7 |
| 3H-3, 145–150 | 21.95 | 7.53 | 6.58 | 35.0 | 558 | 481 | 24.1 | 17.9 | 298 | 116 | 518 | 9.94 | 50.4 | 87 | 25 | 11.1 |
| 4H-3, 145–150 | 31.45 | 7.60 | 7.41 | 35.0 | 563 | 485 | 23.7 | 15.2 | 367 | 89 | 507 | 9.99 | 50.9 | 87 | 26 | 10.8 |
| 5H-3, 145–150 | 40.95 | 7.49 | 7.71 | 35.0 | 564 | 486 | 22.5 | 16.4 | 416 | 79 | 542 | 9.73 | 50.1 | 87 | 29 | 10.8 |
| 6H-3, 145–150 | 50.45 | 7.39 | 8.08 | 35.0 | 562 | 486 | 22.0 | 16.2 | 486 | 76 | 790 | 9.15 | 49.7 | 87 | 30 | 10.3 |
| 9H-3, 145–150 | 78.95 | 7.52 | 8.64 | 34.5 | 558 | 480 | 20.4 | 17.2 | 566 | 58 | 921 | 8.86 | 49.8 | 87 | 33 | 10.4 |
| 12H-3, 145–150 | 107.45 | 7.54 | 8.88 | 35.0 | 555 | 478 | 19.7 | 11.0 | 564 | 52 | 963 | 8.67 | 48.7 | 92 | 39 | 10.0 |
| 15H-3, 145–150 | 135.95 | 7.61 | 9.39 | 34.5 | 551 | 473 | 19.0 | 10.0 | 566 | 63 | 1049 | 9.61 | 47.8 | 92 | 44 | 10.4 |
| 18H-3, 145–150 | 164.45 | 7.54 | 9.02 | 34.0 | 555 | 478 | 19.4 | 8.5 | 546 | 67 | 1130 | 9.97 | 47.5 | 96 | 48 | 10.1 |
| 21X-3, 145–150 | 189.45 | 7.57 | 8.50 | 34.5 | 550 | 469 | 18.4 | 6.5 | 506 | 58 | 976 | 10.5 | 47.8 | 96 | 50 | 9.7 |
| 24X-3, 145–150 | 218.45 | 7.35 | 8.47 | 34.5 | 553 | 471 | 18.7 | 5.7 | 445 | 61 | 1105 | 11.4 | 47.7 | 92 | 54 | 9.6 |
| 27X-3, 145–150 | 247.25 | 7.39 | 7.68 | 34.5 | 552 | 473 | 20.5 | 4.6 | 386 | 56 | 1092 | 11.9 | 47.0 | 96 | 53 | 9.6 |
| 30X-3, 145–150 | 276.15 | 7.57 | 7.35 | 34.5 | 554 | 475 | 21.1 | 3.4 | 332 | 46 | 1066 | 12.2 | 47.1 | 92 | 48 | 9.6 |
| 33X-3, 145–150 | 304.95 | 7.26 | 6.54 | 34.5 | 555 | 475 | 21.1 | 3.5 | 274 | 59 | 1220 | 12.5 | 47.0 | 92 | 47 | 9.8 |

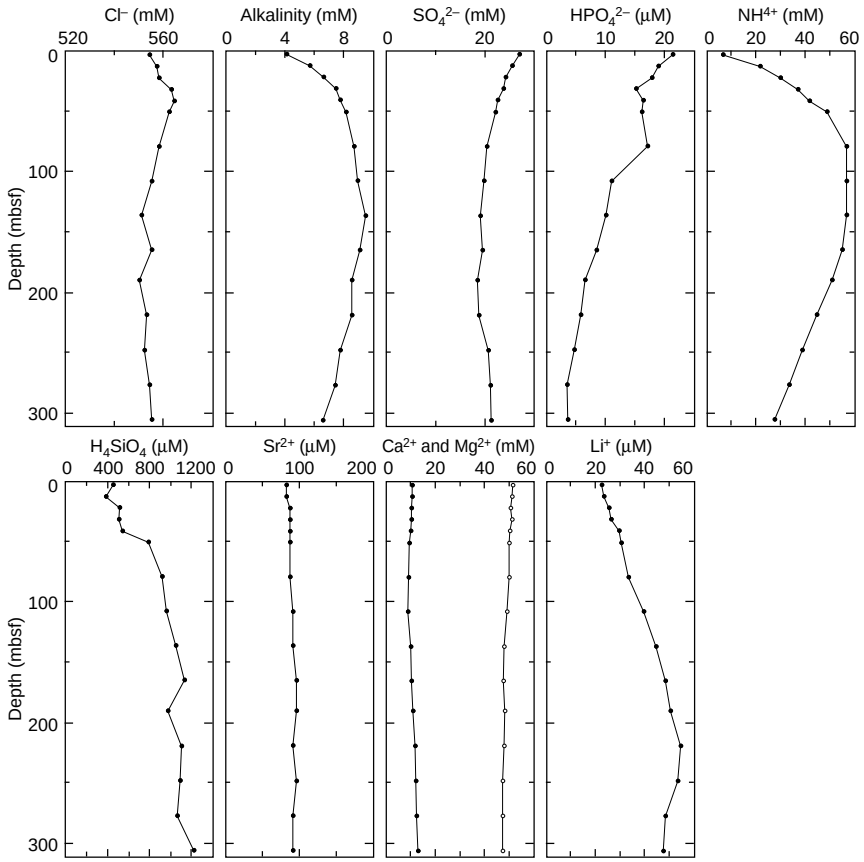


Figure 15. Interstitial water geochemical data, Site 1021. Solid circles = Ca, open circles = Mg.

**Table 14. Concentrations of inorganic carbon, calcium carbonate, total carbon, total organic carbon, total nitrogen, and total sulfur in Hole 1021B.**

| Core, section, interval (cm) | Depth (mbsf) | IC (wt%) | $CaCO_3$ (wt%) | TC (wt%) | TOC (wt%) | TN (wt%) | TS (wt%) | TOC/TN |
|---|---|---|---|---|---|---|---|---|
| 167-1021B- | | | | | | | | |
| 1H-1, 28–29 | 0.28 | 0.07 | 0.6 | 0.72 | 0.65 | 0.14 | 0.09 | 4.64 |
| 1H-3, 28–29 | 3.28 | 1.25 | 10.4 | 2.08 | 0.83 | 0.11 | 0.00 | 7.55 |
| 1H-5, 28–29 | 6.28 | 0.61 | 5.1 | 1.04 | 0.43 | 0.12 | 0.00 | 3.58 |
| 2H-1, 29–30 | 8.29 | 0.06 | 0.5 | 0.57 | 0.51 | 0.15 | 0.00 | 3.40 |
| 2H-3, 29–30 | 11.29 | 0.12 | 1.0 | 0.69 | 0.57 | 0.13 | 0.00 | 4.38 |
| 2H-5, 28–29 | 14.28 | 0.98 | 8.2 | 1.32 | 0.34 | 0.08 | 0.00 | 4.25 |
| 2H-7, 29–30 | 17.29 | 0.81 | 6.7 | 1.31 | 0.50 | 0.12 | 0.00 | 4.17 |
| 3H-2, 30–31 | 19.30 | 0.10 | 0.8 | 0.65 | 0.55 | 0.12 | 0.00 | 4.58 |
| 3H-4, 29–30 | 22.29 | 0.20 | 1.7 | 0.61 | 0.41 | 0.10 | 0.13 | 4.10 |
| 3H-6, 29–30 | 25.29 | 0.08 | 0.7 | 0.47 | 0.39 | 0.11 | 0.00 | 3.55 |

**Only part of this table is produced here. The entire table appears on CD-ROM (back pocket).**

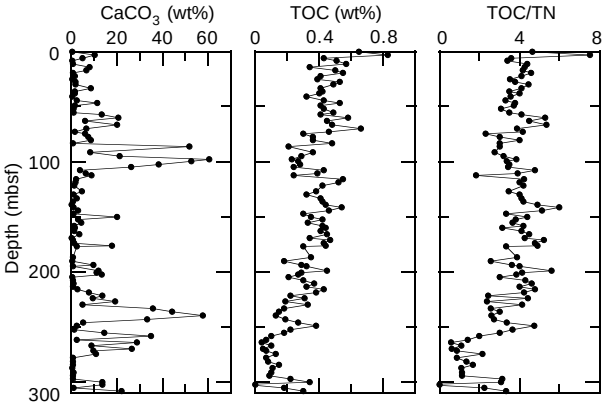


Figure 16. Depth variations of calcium carbonate, total organic carbon (TOC), and total organic carbon/total nitrogen (TOC/TN) in sediments of Hole 1021B.

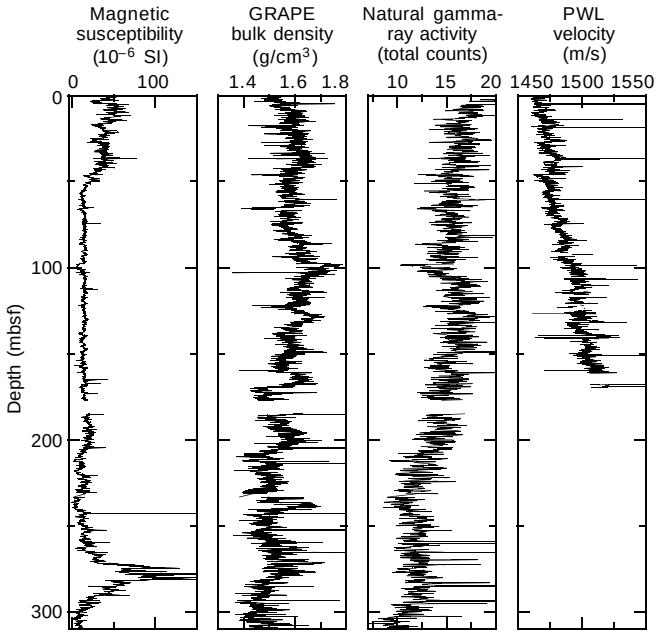


Figure 17. MST data from Hole 1021B.

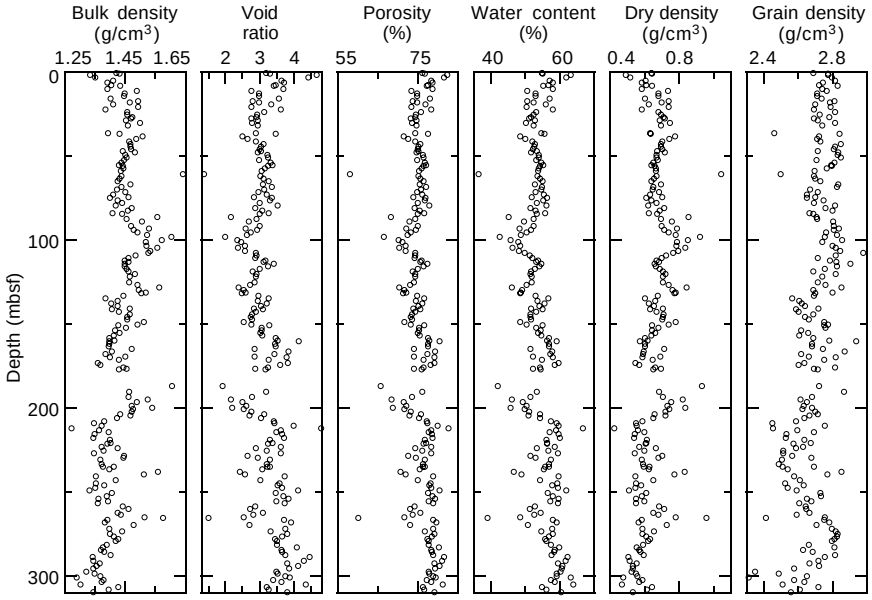


Figure 18. Index property data from Hole 1021B.

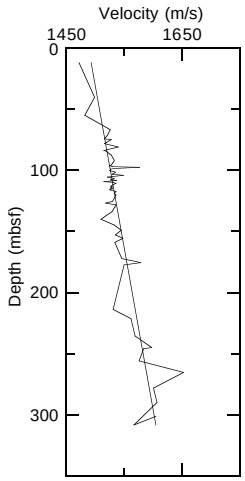


Figure 19. Compressional-wave velocity from Hole 1021B. The line represents the least-squares best fit of all discrete velocity measurements.

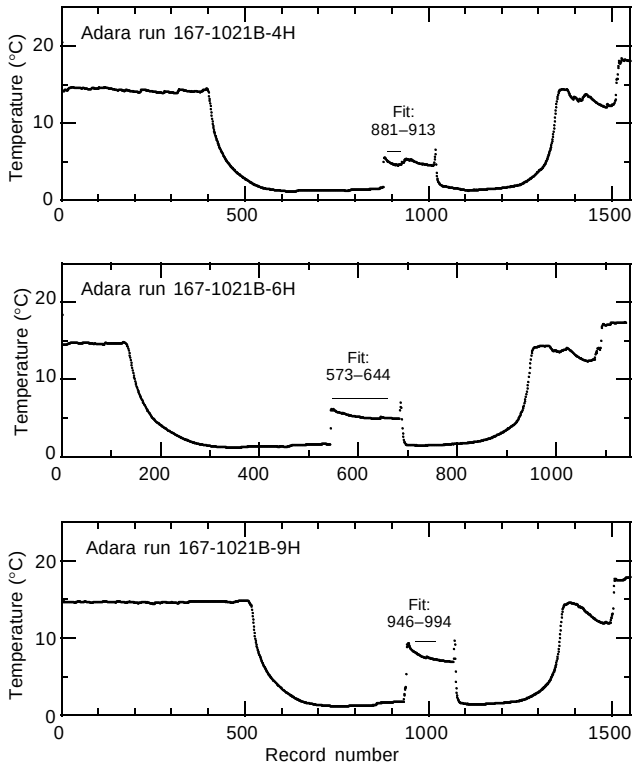


Figure 20. Hole 1021B downhole temperature vs. record number (5-s recording frequency) for each measurement run, showing the intervals fitted to determine the downhole temperature.

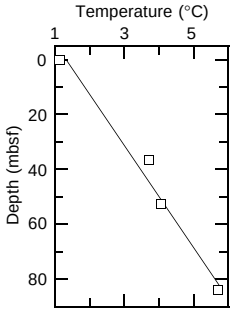


Figure 21. Downhole temperature gradient for Hole 1021B.

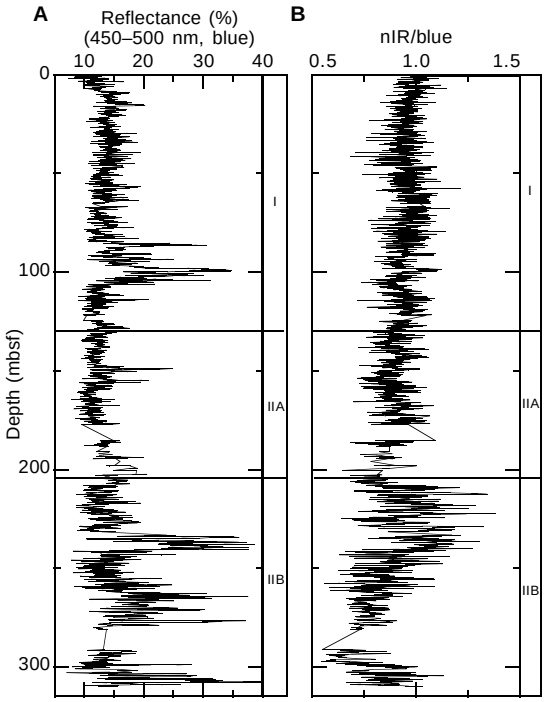


Figure 22. Summary of color reflectance data for Hole 1021A compared to major lithostratigraphic units. **A.** Percent reflectance for 450–500-nm band average (blue). **B.** Ratio of 850–900-nm band average (near infrared) to blue.

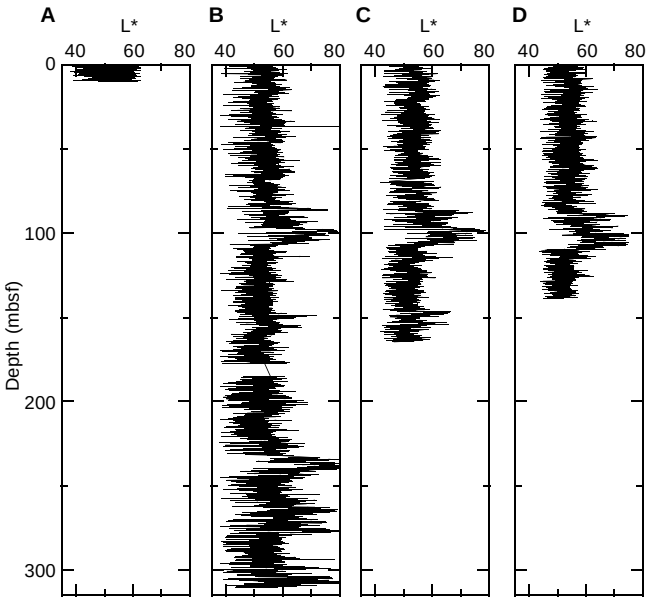


Figure 23. Intensity of color CIELAB L* from Holes (**A**) 1021A, (**B**) 1021B, (**C**) 1021C, and (**D**) 1021D. Data were decimated at 2-cm intervals.

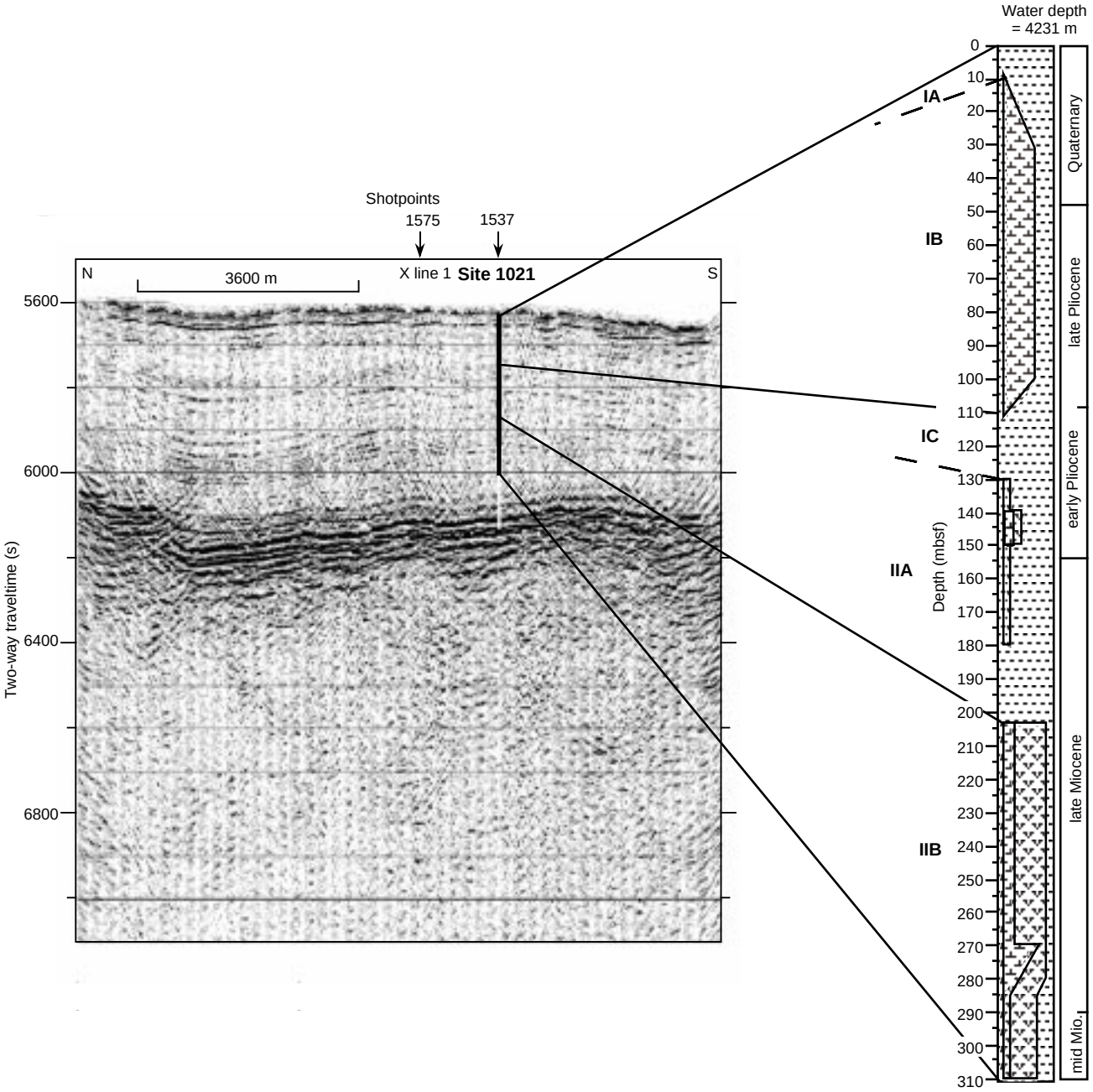


Figure 24. Comparison of the lithostratigraphic column at Site 1021 and a seismic reflection profile through it (Line EW9504 CA5-4; Lyle et al., 1995a, 1995b). Ties are calculated from shipboard seismic velocity measurements (see “Physical Properties” section, this chapter). On y-axis, (s) = milliseconds.